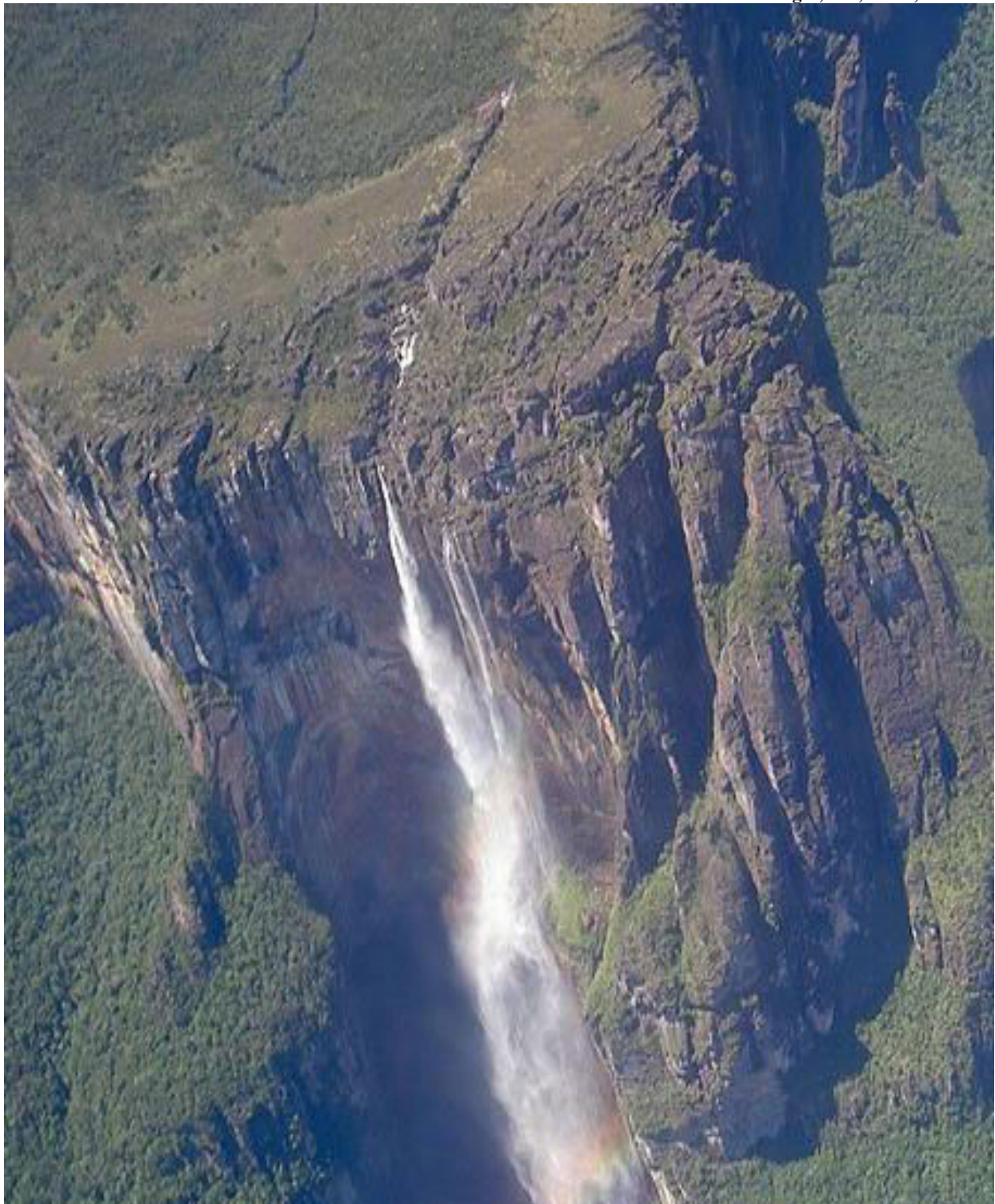# QUANTITATIVE ANALYSIS OF TECTONICALLY UPLIFTED TOPOGRAPHY

Dr. N.L. Dongre, IPS, Ph.D., DLitt

The Pachmarhi hills exhibit dynamics of Geomorphic process and the effect of initial surface organization of Tectonic uplift.

Abstract: *It is presented that the results of an experimental study of topography dynamics under conditions of constant precipitation and uplift rate. The experiment is designed to develop a complete drainage network by the growth and propagation of erosion instabilities in response to tectonic perturbations. The quantitative analysis of topographic evolution is made possible by using telemetric lasers that perform elevation measurements at an excellent level of precision. .The study is focused on the effect of initial surface organization and of uplift rate on both the transient dynamics and the steady state forms of topography. It is shown that the transient phase is strongly dependent on the initial internally drained area, which is found to decrease exponentially with time. The topography always reaches a steady state whose mean elevation depends linearly on uplift rate with a strictly positive value when uplift is zero. Steady state surfaces are characterized by a well-defined slope-area power law with a constant exponent of —0.12 and amplitude that depends linearly on uplift rate with a strictly positive value when uplift is zero. These results are consistent with a stream power law erosion model that includes a non-negligible threshold for particle detachment. Uncertainty regarding the sediment transport length is resolved by calibrating the transient dynamics with a surface process model. Reappraising published results on the linear dependency between mean elevation, or relief, and denudation rate, it is suggested that an erosion threshold is worth considering for large-scale systems.*

KEYWORDS: *landscape evolution, topography, relief, experimental modeling, tectonic geomorphology, numerical modeling*

Introduction

[2] The understanding of the long term dynamics of the Earth's topography is based mainly on the results of theoretical analysis and numerical models [*Braun and Sam-bridge,* 1997; *Davy and Crave,* 2000; *Howard et al.,* 1994; *Kirkby,* 1971; *Kooi and Beaumont,* 1996; *Willgoose et al.,* 1991b], for which few constraints exist to validate the macroscopic evolution, and the characteristics of simulated topographies. For instance, most studies refer to the stream-power model to simulate erosion fluxes, arguing that topographic measures such as slope and drainage area are consistent with this model. But this consistency is theoretically valid in conditions that are difficult to demonstrate in natural systems (dynamic equilibrium, known field of precipitation of uplift and of erodibility). Moreover the relationship between given erosion law and the local measures of topography are equivocal in conditions of dynamical equilibrium: it depends on the way the sediment is transported in rivers whose two classical end-member processes are detachment-limited and transport-limited. Only a thorough analysis of the transient stages can discriminate between these sediment transport processes [*Tucker and Whipple,* 2002; *Whipple and Tucker,* 2002]. Another important issue concerns the often overlooked importance of a non-negligible threshold of transport and/ or bed erosion [*Howard,* 1980, 1994; *Snyder,* 2001; *Talling,* 2000] that have important implications for landscape dynamics [*Densmore et al.,* 1998; *Molnar,* 2001; *Rinaldo et al.* , 1995; *Tucker and Bras,* 2000; *Tucker and Slinger-land,* 1997], and for the scaling of relief with uplift rate [*Snyder et al.,* 2002].

[3] Assessing erosion processes from natural geomorphic systems is really a difficult challenge considering the uncertainties about boundary conditions, and flux measurements. The experimental approach is an interesting substitute for studying such complex processes, in which boundary conditions can be perfectly controlled and topography variations continuously surveyed. In comparison to other domains of Earth sciences [*Davy and Cobbold,* 1991], the experimental approach remains relatively uncommon in studying the dynamic of geomorphic systems [*Schumm et al.,* 1987]. In theory, it is possible to reproduce large-scale systems with small-scale experiments, provided that the reduction in length and in time-scales preserves the basic dimensionless equations. As for many natural processes, the little is known about the dynamics of geomorphic processes already shows that natural large-scale conditions cannot be perfectly down-scaled in the laboratory. A specific problem for hydraulically driven erosion systems is the co-existence of short timescales for hydraulics, and long timescales for tectonics, so that a perfect downscaling of the whole range of pertinent timescales is nearly impossible. That is why many studies have focused on the dynamics of one elementary process and tried to keep a strong degree of similarity between the natural system and the laboratory: channel dynamics [*Gardner,* 1983; *Holland and Pickup,* 1976; *Sheperd and Schumm,* 1974], bedrock experiments [*Thompson and Wohl,* 1998], sediment transport mechanics [*Paola et al.,* 1992], terrace formation [*Mizutani,* 1998], meander evolution [*Smith,* 1998], hillslope evolution [*Den-smore et al.,* 1997; *Roering et al.,* 2001], floodplain dynamics [*Ashmore,* 1982; *Meunier and Metivier,* 2000; *Wood et al.,* 1993] or alluvial fan formation [*Whipple et*

Table 1. Main Characteristics of Previous Experimental Studies on the Dynamic of Drainage Basins and Topography

		Model Characteristics			Material		Measurements		
		Model Size,	Droplet Size,	Tectonic		D_{50},	Topography		Sediment
Reference	Scientific Question	cm	mm	Forcing[a]	Type	mm	Method	Resolution	flux
Flint, 1973	Drainage network development	29 ×45 × 16	<0.5	R	soil (?)	0.06–0.016	reference grid	2D, >1 cm[b]	. . .
Schumm et al., 1987	Basin dynamics, drainage networks	900 × 1500 ×200	1.52–3.7	R,T	loamy sand	0.3	mobile point gauge	2D, >1 cm[b]	manual samples
Phillips and Schumm, 1987	Drainage network development	200×300 × 20	<1[b]	R	sand, silt, clay	0.2	topography profiles	?	. . .
Wittmann et al., 1991	Fractal properties of drainage networks	Ø 140×9	<1[b]	R	sand	0.18	photo	. . .	. . .
Czirok et al., 1993	Fractal properties of topography	18 × 60 ×4	<1[b]	R	sand, soil	0.15	cross sect. photo	1D, 0.5 mm[b]	. . .
Hancock and Willgoose, 2001b	Validation of numerical model	150 ×150 ×50	0.134	R	fly ash	0.016	digital photogramme try[c]	2D, 6 mm	manual samples
Crave et al., 2000	Topography dynamics	18 × 27 × 4	0.02–0.05	R	silica	0.01	telemetric lasers	2D, 1 mm	. . .
Hasbargen and Paola, 2000	Stability of steadystate topography	Ø 100 ×100	<0.2	T	silica, kaolinite	0.045	photo	. . .	regular samples
This study	Landscape response to tectonic uplift	20 × 30 ×9	0.05–0.09	R,T	loess	0.045	telemetric lasers	2D, 1 mm	. . .

[a]R, relaxation experiments; T, continuous uplift experiment.
[b]Estimated value.
[c]*Hancock and Willgoose* [2001a].

*al.,*1998]. Conversely many authors chose to study systems that are not perfect natural analogs, but which exhibit qualitatively similar dynamics in their interaction between the experimental "hillslopes" and "channels". These studies (Table 1) include the study of river network development [*Flint,* 1973; *Schumm t al.,* 1987], the fractal properties of evolving topographies [*Czirok t al.,* 1993; *Wittmann t al.,* 1991], the landscape development in relaxation [*Crav t al.,* 2000; *Hancock and Willgoos* , 2001a, 2001b] or under constant rates of uplift and rainfall [*Hasbarg n and Paola,* 2000]. Numerous results have influenced or revised our views on the transient dynamic of watersheds, but most of them remain qualitative in essence because (1) the elementary processes were not really calibrated and (2) the topography and sediment fluxes were not sufficiently documented.

 I have built a new experimental setup that aims to improve previous experimental studies by sampling topographic data at very high resolution. This technical enhancement makes possible the measurement of

local erosion fluxes from topographic records and thus the derivation of an erosion law. [4] The experimental strategy was as follows:

1. It was chosen to generate water flow from a rain device in order to mimic the natural tendency of drainage networks to develop in response to the growth and capture of incisions. In particular, the surface of the experiment organizes itself into a wide range of drainage basins whose area lies from 0 to about 1/10th of system size. It is believed that the mechanisms that make this area distribution are key elements of the global system dynamics.

2. It is expected that the drainage organization to depend on the initial topography. Thus the experiments are made with different initial topographies, considering that the role of this parameter on the global dynamics is worth being studied.
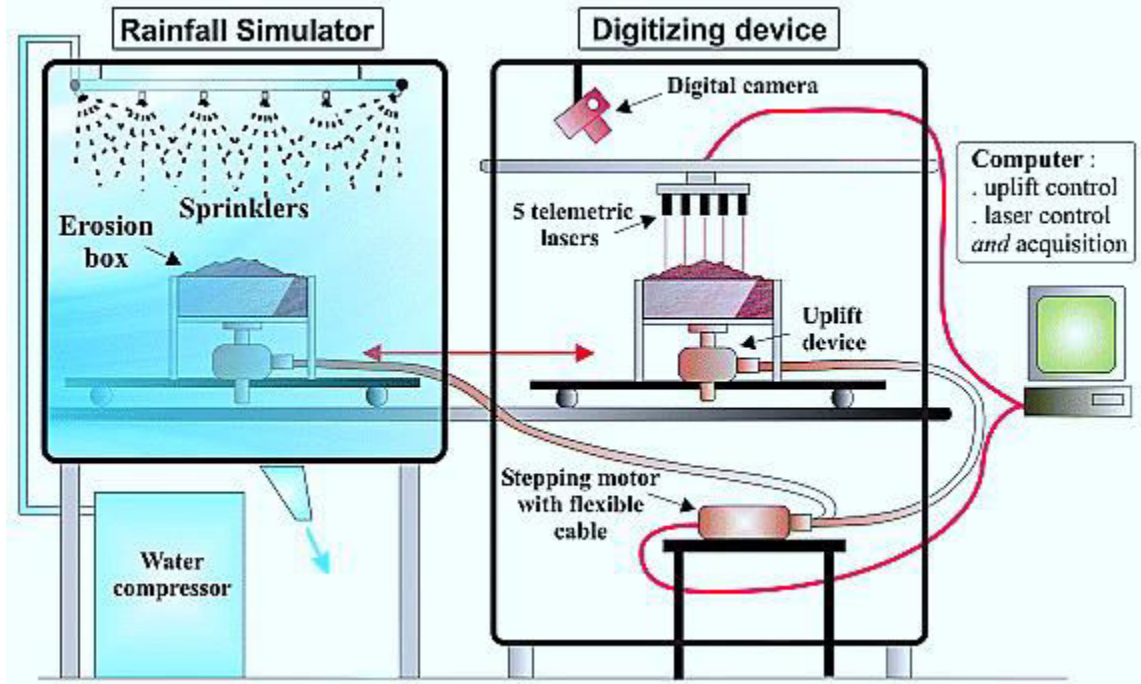

Figure 1. Experimental setup.(after Dimitri Lague,Alain Crave ,and Philippe Davy)

3. Each experiment run-up is let to a dynamic equilibrium between erosion and uplift rates. Under this condition the slope-area relationship that characterizes topography can be interpreted in terms of an erosion law *[Howard,* 1980; *Willgoose et al.,* 1991a]. As developed by *Whipple and Tucker* [2002], there is likely a whole family of erosion models that would be consistent with the experimental findings, in particular models in which detachment rate is a function of sediment flux [*Howard,* 1998; *Sklar and Dietrich,* 1998, 2001]. Given the uncertainties on the sediment erosion-transport dynamics at the model scale, the simplest heuristic erosion model is sought that depends only on local slope S and water flow Q_w. One important reason for this is that only these two parameters can be measured from topography assuming that drainage area is a surrogate variable for Q_w. But it is recognized that this parameterization might encompass more complex processes with, for instance, a dependency on sediment flux [*Sklar and Dietrich,* 1998, 2001; *Whipple and Tucker,* 2002]. Since it is found that a power law dependency on both Q_w and S, it is hereafter called this model a "stream power law".

4. At steady state, the slope distribution is intimately related to the applied uplift [*Lague et al.,* 2000; *Snyder et al.*, 2000; *Whipple and Tucker,* 1999]. Thus expect to derive the slope parameters of the erosion law, as well as the eventual detachment threshold *[Snyder et al.,* 2002], by performing experiments at different uplift rates. The dependence of the erosion law on water flow is assumed to come directly from the relationship between sediment flux and drainage area.

4

[5] Beyond the determination of the erosion law, the experiments are powerful tools to understand topographic dynamics during the transient stages. It is especially focused on the evolution of topographic forms as representative of erosion instabilities and on characteristic timescales, as well as on their relationship with experimental boundary conditions and erosion parameters. Moreover a complete description of the erosion law cannot be achieved without examining transient stages [*Tucker and Whipple*, 2002; *Whipple and Tucker,* 2002]. This is the case for the distance over which sediments are transported, which is one major parameter of transport process that controls both transient evolution and eventual topographic form [*Davy and Crave,* 2000; *Kooi and Beaumont,* 1996; *Whipple and Tucker,* 2002]. The analysis of transient stages is not as straightforward as the analysis of equilibrium stages. Thus it is carried out a preliminary comparison between experiments and numerical results from a process-based model [*Crave and Davy,* 2001; *Davy and Crave,* 2000].

[6] Finally, the degree of analogy of the experiments with natural systems is discussed. Though the analogy is obviously incomplete, some qualitative consequences relevant to continental scale dynamics can be drawn from our experimental findings, in particular regarding the existence of a non-negligible threshold of bed erosion and/or sediment transport, and the role of initial conditions and uplift rate on landscape dynamics.

2. Experimental Setup and Methods

2.1. Facilities and Material

[7] The experimental system consists of three components: (i) a rainfall simulator (called the "fog box"), (ii) a monitoring device (digitization, pictures) and (iii) an erosion box that can move between the two previous devices on a mobile tray (Figure 1). The opacity and hygrometry of the "fog box" make the use of a separate system for data acquisition necessary.

[8] Two major constraints have governed the design of the system: the need for accurate and frequent acquisitions of digital topography (DEM) of the experiments, and the limitation of the splash effect at droplet impact in order to reduce the transport processes to surface water flow. The precipitation simulator consists of a high-pressure spray system of sixteen nozzles (Fog System by Dutrie) placed into a closed transparent box of 2 x 2 x 2 m. The range of mean droplet diameter varies between 5 and 9 mm with water pressure. Various surface precipitation rates are obtained by changing water pressure, nozzle height or nozzle configuration. For the set of experiments reported here, the precipitation distribution was kept constant and spatially uniform with an average precipitation rate equal to 100 ± 15mm h^{-1}.

[9] Special attention is paid to topographic measurements that must be both accurate and fast, in order to produce high resolution Digital Elevation Models (DEMs) in a short time lapse. First a stereo-photography approach was tried, but it results in DEMs that have too much imprecision and that are very sensitive to shadow effects around vertical slopes. Thus an automated digitizing device of 5 telemetric lasers, mounted on a rack, and precisely controlled by stepping-motors aligned along the horizontal axes was designed and built. This method produces high-resolution DEMs that are almost insensitive to shadow effects, with a vertical accuracy of 40 μm and a minimum horizontal resolution of 1 mm (limited by the laser spot size). The horizontal resolution (e.g., pixel size of DEM) is also constrained by the need to minimize acquisition time. For a 20 x 30 cm experiment, the acquisition time is about 6 min. It was checked that interrupting the experiments during this time lapse does not affect the model evolution by comparing with a continuously eroded model. Compared to previous similar work (Table 1) for which best pixel size and vertical accuracy were respectively 1 cm, and 0.6 cm (stereo photography *[Hancock and Will-gose,* 2001a, 2001b]), this device proved to be a noticeable advance.

[10] The choice of experimental material is crucial since it basically predetermines the erosion and transport laws. Table 1 summarizes the materials used by various authors. All chosen materials have small grain size, thus small shear strengths that make possible the erosion and transport by small water fluxes. The appearance of interparticle cohesion in very fine powder fixes a limit in decreasing grain size. On the other hand, cohesion allows the development of a finely incised drainage network with steep slopes.

[11] I have selected a natural loess soil that has been crushed and sieved to reach a D_{50} of 20 μm ($D_{10} = 4$

μm, and D_{90} = 43 μm). It is composed mainly of quartz, mica and less than 10% percent of clay (chlorites) which ensures a small grain-to-grain cohesion. Its density is around 2700 kg.m^{-3}.

[12] The erosion box is a 20 x 30 x 10 cm box made of transparent Plexiglas. A movable bottom lifted by a stepping motor simulates a spatially uniform uplift, with computer-controlled rates ranging from 0.5 to 5 cm h^{-1}. The mechanical assembly guarantees smooth movements of the base. The four box walls act as boundary conditions of the eroding system with constant elevation. Unlike the mechanism used by *Hasbargen and Paola* [2000], and *Hancock and Willgoose* [2001a, 2001b] the device prevents box walls from concentrating water on these boundaries. It also maintains a constant distance between nozzles and the eroded surface at dynamic equilibrium reached toward the end of our experiments.

2.2. Erosion Processes

[13] The primary objective was to simulate the evolution of a surface on which particle detachment and transport occurs mainly by surface runoff, so that it required to reduce as far as possible the detachment effect of droplet impacts. It has been experimentally demonstrated that the detachment of soil by splash effect on a horizontal surface occurs if the critical raindrop kinetic energy is larger than the grain-grain binding energy characterized by soil shear strength *[Salles et al.,* 2000; *Sharma et al.,* 1991]. The measured range of kinetic energy threshold varies between 5 and 600 μJ, depending on the material grain size *[Salles et al.,*2000], the bulk density, the water content and the clay content *[Sharma et al.,* 1991]. Given a maximum raindrop diameter of 20 μm and a maximum impact velocity of 10 m.s^{-1}, the impact kinetic energy that might possibly occur in the fog box is of the order of 10^{-4} μJ, and is much smaller than the grain-grain binding energy. Thus no detachment can occur by this process on the experiments, and the driving force for detaching and transporting particles is only overland flow.

[14] Because of the fog opacity and the small size of the experiment, it is not possible to make direct observation or measurements of water and sediment flows, and thus a quantitative estimate of the sediment-transport modes (bed, mixed can be estimated at steady state, that is when erosion totally compensates uplift: $Q_s = UA$ and $Q_w = pA$, where U is uplift rate, A is drainage area and p is precipitation rate (note that infiltration rate is negligible). The volumetric concentration of particles, $C_v = Q_s/Q_w = U/p$, *is* theoretically spatially uniform. In this experiments, the uplift rates range between 5 and 50 mm h^{-1}, corresponding to volumetric concentrations varying between 5 and 50%. Thus, the sediment concentration ranges from fluvial-like values (<10 -20%), to mudflow ones (that is a hypercon-centrated flow of very fine particles *[Coussot,* 1997]) where the particle interactions makes the flow rheology significantly different from the one of pure water. A consequence is that, the stream power law model developed for fluvial sediment transport and bedrock river incision *[Howard,* 1980, 1994] might not be applicable for the upper range of sediment concentrations. However, little is known on bed erosion and sediment transport by mudflows, and I cannot predict a priori what would the difference between top-ographies shaped by runoff erosion and by mudflow.

[15] In the case of low sediment concentration, the flow regime is characterized by Froude and Reynolds numbers that depend on the flow velocity u (ranging between 0.001 and 0.1 m.s^{-1}), on the hydraulic radius R (which is about the flow height, 0.1 -2 mm) and on the kinematic viscosity of the sediment mixture. v If the kinematic viscosity is taken as that of pure water, the Froude number F_r lies in the range 0.01 and 3 (sub to super critical flow) and the Reynolds number R_e is 200 maximum (laminar flow). In the case of mudflow, the mixture kinematic viscosity is much larger (up to 1000 times the viscosity of clear water *[Coussot,* 1997]), the flow is likely to be strongly laminar with Reynolds numbers possibly smaller than 1.

[16] Particle fall velocity is likely to be very low because particle size is very small, and because sediment mixture viscosity may be quite large for high sediment concentration *[Coussot,* 1997]. It is thus likely that, once a particle enters into the suspension flow, it is re-deposited far from its source. However, as observed in the experiments by *Whip-ple et al.* [1998], flows with very low Reynolds number can leave particles near the bed while, in theory, they should have been transported in a suspended mode. Thus there was not a priori clue to whether the main transport mode is suspended or bed load, or mixed. Experiments on a micro flume are planned in order to better understand the sediment transport mode.

Table 2. Experimental Conditions and Results

Experiment	Initial Surface	Uplift Rate, cm h^{-1}	Nb DEMs	C_s,ini, %	τ_c, min	$\langle h \rangle_{\text{ini}}$, cm	$\langle h \rangle_{\text{lim}}^{\text{obs}}$, cm	τ_h, min	$\langle h \rangle_{\text{lim}}^{\text{fit}}$, cm
RR1	Random	0	9	8	9.6 ± 0.2	3.01	1.08	17 ± 3	0.98 ± 0.11
RR2	Random	0	11	25	8.9 ± 0.2	2.03	1.15	65.3 ± 24	1.02 ± 0.02
RR3	Random	0	17	5	5.4 ± 0.3	2.93	0.90	20 ± 2a	0.98 ± 0.02a
RE1	Eroded	0	8	100	NA	2.91	1.14	10.6 ± 0.4	1.11 ± 0.02
RE2	Eroded	0	8	100	NA	3.34	1.16	12.5 ± 0.3	1.02 ± 0.02
RE3	Eroded	0	10	100	NA	4.07	0.99	12.5 ± 0.5	0.94 ± 0.03
CR1	Random	5	26	41	11.8 ± 0.4	0.94	3.18 ± 0.03b	31.6 ±1.9a	4.16 ± 0.12a
CR2	Random	2	21	75	10.8 ± 0.3	1.00	1.97 ± 0.09b	28.8 ± 1.6a	2.13 ± 0.04a
CR3	Random	1	13	20	12.9 ± 0.4	0.79	1.58 ± 0.03b	26.7 ± 2.6a	1.58 ± 0.04a
CR4	Random	0.5	9	43	14.5 ± 0.5	0.84	1.39 ± 0.03b	NA^c	NA^c
CE1	Eroded	3	13	100	NA	1.44	2.30 ± 0.04b	NA^d	NA^d
CE2	Eroded	2	13	100	NA	1.57	1.87 ± 0.06c	13.0 ± 1.8	1.90 ± 0.03

[a]Determined from exponential fit for $C_s > 99\%$.
[b]Average of the mean surface elevation of the last three stages. Error is standard deviation.
[c]Record failure at the beginning of the experiment.
[d]Nonexponential evolution.

[17] Mass movements of small amplitude were observed near the box boundaries during the early stages of surface evolution. However, in comparison to runoff erosion and transport the corresponding flux is negligible.

2.3. Experimental Protocol

[18] For each experimental run, a known and constant weight of material is poured in the erosion box, slightly compacted and wetted until saturation is reached to ensure a steady state and uniform infiltration rate during the run. An initial surface is then formed by randomly pouring material in order to generate a surface with a roughness (standard deviation of the elevation) ranging from 0.3 to 0.9 mm. During the experiments, photography and DEM acquisition are performed at intervals which depend on the rate of surface change (e.g., between 3 and 40 min), generating at least 8 and up to 26 stages of surface records (Table 2). Results from 12 experiments are reported in this study. These are grouped into 2 main thematic series as a function of the uplift input history: (i) relaxation experiments (series R, 6 experiments) for which the initial surface is uplifted first, and evolved afterward by the sole effect of erosion, and (ii) continuous uplift experiments (series C, 6 experiments) on which a spatially uniform uplift is applied. The initial surface was either random (series RR and CR) or shaped during an earlier experiment (series RE and CE). In the latter case, the initial drainage area is entirely connected to boundary conditions; The term "eroded" was used to designate these initial topographic conditions. Various uplift step (series R) or uplift rate (series C) were studied (Table 2). Other experimental inputs (precipitation rate, material type) were held constant.

2.4. Topographic Analysis

[19] For the macroscopic description of the system, it is computed that the mean elevation and the area of the surface which effectively contributes to outflow. The latter parameter is defined as the surface percentage hydraulically connected to system boundaries; it is called C_S, the surface connectivity. C_S is computed from the DEM using a numerical code analogous to the walker model developed by *Darboux et al.* [2002] for which a given rain amount is poured on top of the surface that either fills surface holes or runs to boundary conditions. C_s is equal to the flow ratio that runs outside; it is calculated by applying a "rainfall" equal to the vertical accuracy of laser measurements (e.g., 100 μm) in order to fill the holes due to DEM errors.

[20] For steady state topographies, the detailed features of the surface were characterized using the length-area scaling relationship (also known as *Hack*'s [1957] law, when it is a power law relationship)

and the area-slope relationship *[Flint, 1974; Hack, 1957; Howard, 1 9 8 0 ; Howard and Kerby,* 1983; *Ijjasz-Vasquez and Bras,* 1995; *Lague et al.,* 2000; *Moglen and Bras,* 1995; *Montgomery,* 2001; *Montgomery and Foufoula-Georgiou,* 1993; *Sklar and Dietrich,* 1998; *Snyder et al.,* 2000; *Tarboton et al.,* 1989, 1992; *Tucker and Bras,* 1998; *Whipple and Tucker,* 1999, 2002; *Willgoose et al.,* 1991a]. Hack's law is adequately modeled by a power law between mainstream length and drainage area whose exponent characterizes the degree of flow convergence *[Rigon et al.,* 1996]. The area-slope relationship is also found to be a power law, whose expression at steady state is expected to depend solely on the erosion-transport processes and on uplift rate for the experimental conditions *[Howard,* 1980; *Lague et al.,* 2000; *Snyder et al.,* 2000; *Tucker and Bras,* 1998; *Whipple and Tucker,* 1999, 2002; *Willgoose et al.,* 1991a]. Drainage area is computed using a D8 drainage routing algorithm of convergent flow, and local slope is calculated over two adjacent pixels in the steepest direction (e.g., over a constant horizontal length of 1 mm). When plotting the area-slope points for the whole surface at steady state, one observes a large data scatter which is related to (1) locally incomplete steady state, or (2) to spatial variability of material property and rainfall intensity *[Moglen and Bras,* 1995], or (3) to small DEM errors which affect local slope measurement and drainage area calculation *[Lague et al., 2 0 0 0].* In particular, the D8 drainage routing algorithm assumes that the network has a tree-like organization, and that the flow width is less than, or equal to, one DEM grid cell (i.e., 1mm). The main errors come from low-slope areas close to boundary conditions where flow width is generally large. Since the D-8 algorithm concentrates the flow in one pixel, it assigns artificially low drainage values to some pixels that are actually shaped by large flows. This could potentially influence the slope -area regressions, by decreasing the apparent value of the power law exponent 9. The quantitative estimation of this bias is difficult as the definition of flow width is not always obvious on experimental surfaces, especially when the flow is barely channelized. However, as it will be shown in this paper, the slope-area exponent is roughly constant for all experimental conditions, whether the flow is deeply channelized or not (compare photographs *F* on Figure 3 a, $U = 0\,cm\ h^{-1}$ and Figure 7a, $U = 5\,cm\ h^{-1}$). Hence, it is guessed that the bias induced by using a D8 algorithm is low. It was quantitatively checked that this effect by using a Dinf algorithm (TauDEM program by *Tarboton* [1997]) in an unchanneled case (which is the most unfavorable case for the D8 algorithm). And I did not find significant differences in the slope-area calculated exponents (D8: $\theta = 0.13$, Dinf: $\theta = 0.14$).

[21] The large scatter in the slope-area diagram is smoothed by averaging slope in logarithmically spaced intervals of drainage area. The same method is applied to the mainstream length for Hack's law. The parameters of the power laws are estimated from these averaged relationships.

3. Experimental Results on Transient Dynamics
3.1. Relaxation Experiments
[22] In this section, the evolution of two experiments that differ from their initial surface shape (Plateau with either a random roughness or an "eroded" topography) is described. For both experiments, the initial boundary conditions are near-vertical edges, and time zero corresponds to the onset of precipitation. The experiments allow to specifically study the impact of initial conditions on the macroscopic evolution.

3.1.1. Random Initial Topography
[23] The sequence of photographs (Figure 2a) shows that, rapidly after the beginning of the experiment (stage A), small parallel incisions initiate at the boundaries (stage B). These incisions propagate upstream perpendicularly to the plateau edge and progressively individualize into a deeply incised, arborescent valley network (stage C). Downstream of the incisions, the topographic slopes decrease gently with a very finely imprinted drainage network. During further incision, crest lines progressively establish diagonally from each corner (stage D). After ~50 min, the plateau is completely dissected (stage E) and the topography declines slowly toward a state of no erosion (stage F). In plain view, the drainage network remains approximately stable during this last phase
[24] For the first 50 min, the sequence of cross-section evolution (Figure 2b) shows that (1) the initial plateau is progressively cut into, (2) the actively eroded zone is mostly
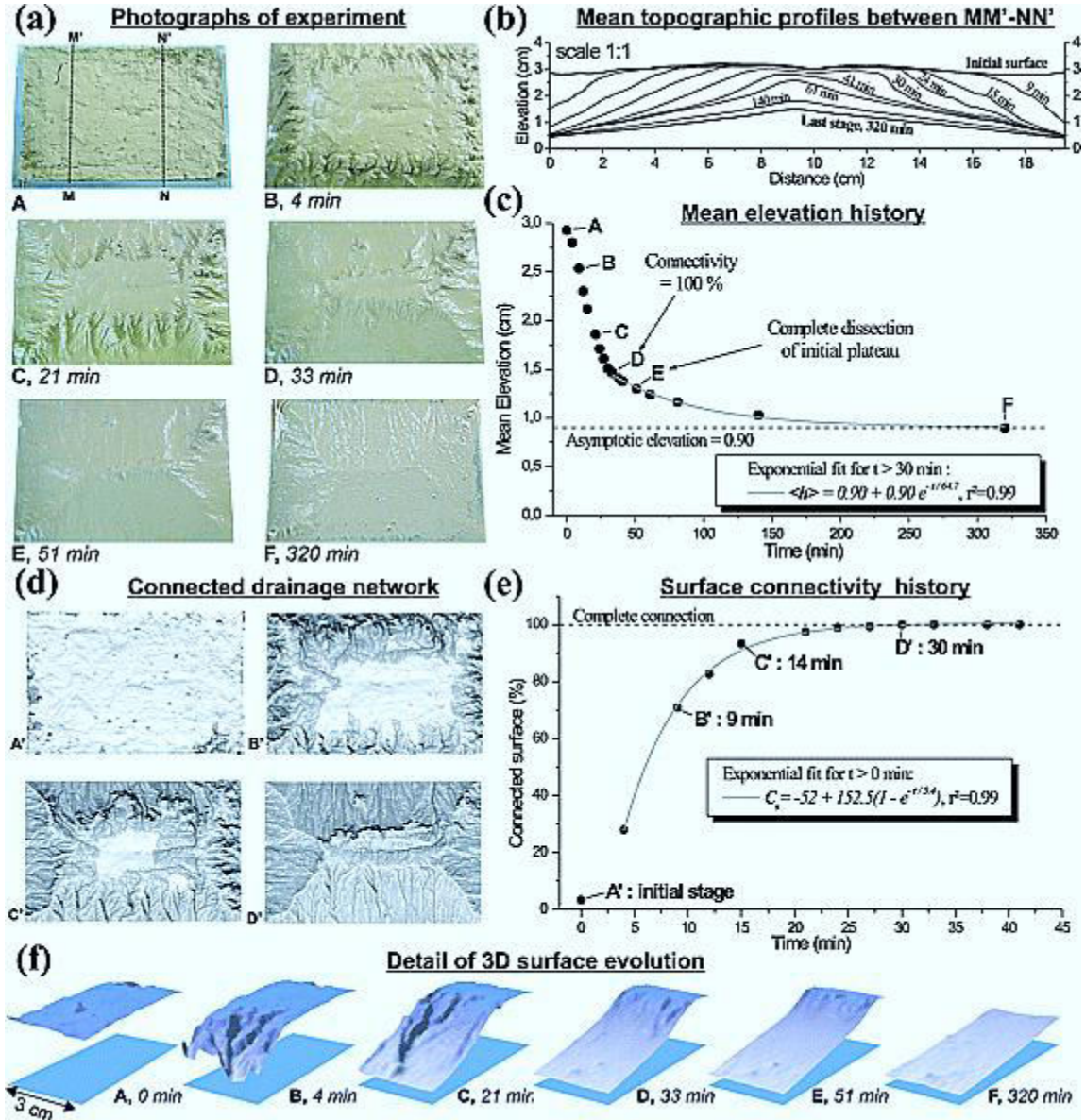
Figure 2. Relaxation experiment with random topography (RR3 experiment).

straight or concave with a slope that is progressively decreasing, and (3) a stable profile, with no net erosion, grows inward from the downstream boundaries. After ~60 min, the initial plateau totally disappears, and the whole topographic profile decreases quite homogeneously down to the eventual stable profile.

[25] Macroscopically, the mean surface elevation continuously decreases with two different phases of evolution (Figure 2c): during the first 30 min, mean elevation decreases almost linearly (stages A, B, C, D), while after 30 min, it decreases exponentially toward a final elevation of 0.90 cm:

$$\langle h \rangle(t) = \langle h \rangle_{\text{limit}} + (\langle h \rangle(t_0) - \langle h \rangle_{\text{limit}})\exp\left(-\frac{t-t_0}{\tau h}\right) \qquad (1)$$

with $\langle h \rangle(t)$ the mean elevation, t_o any time at which the exponential model is valid, $\langle h \rangle_{\text{limit}}$ the final elevation at infinite time, and τ_h the characteristic timescale of the exponential decrease (stages E,F). The first phase erodes almost 75% of the total eroded volume during one tenth of the experiment duration. Note that the total disappearance of the initial plateau (stage E) occurs 20-30 min later than the beginning

9

of the exponentially decreasing phase (stage D), and it does not correspond to any particular change of the mean elevation evolution.

[26] Surface connectivity (Figures 2d and 2e) increases approximately exponentially, starting from 3% of connected surface toward complete connectivity (stage D′), with a characteristic time of about 5 min. Spatial distribution of connected surface (Figure 2d) shows that the connectivity increase is not spatially uniform, and that the unconnected area does not form a contiguous zone. Connectivity growth proceeds by capture of internally drained areas by the growing incisions, with numerous drainage network reorganizations. The complete connection is achieved after 30 min, right at the transition between the two phases of the mean elevation evolution (stage D, Figure 2c). This suggests that surface connectivity exerts a major control on the macroscopic experiment evolution.
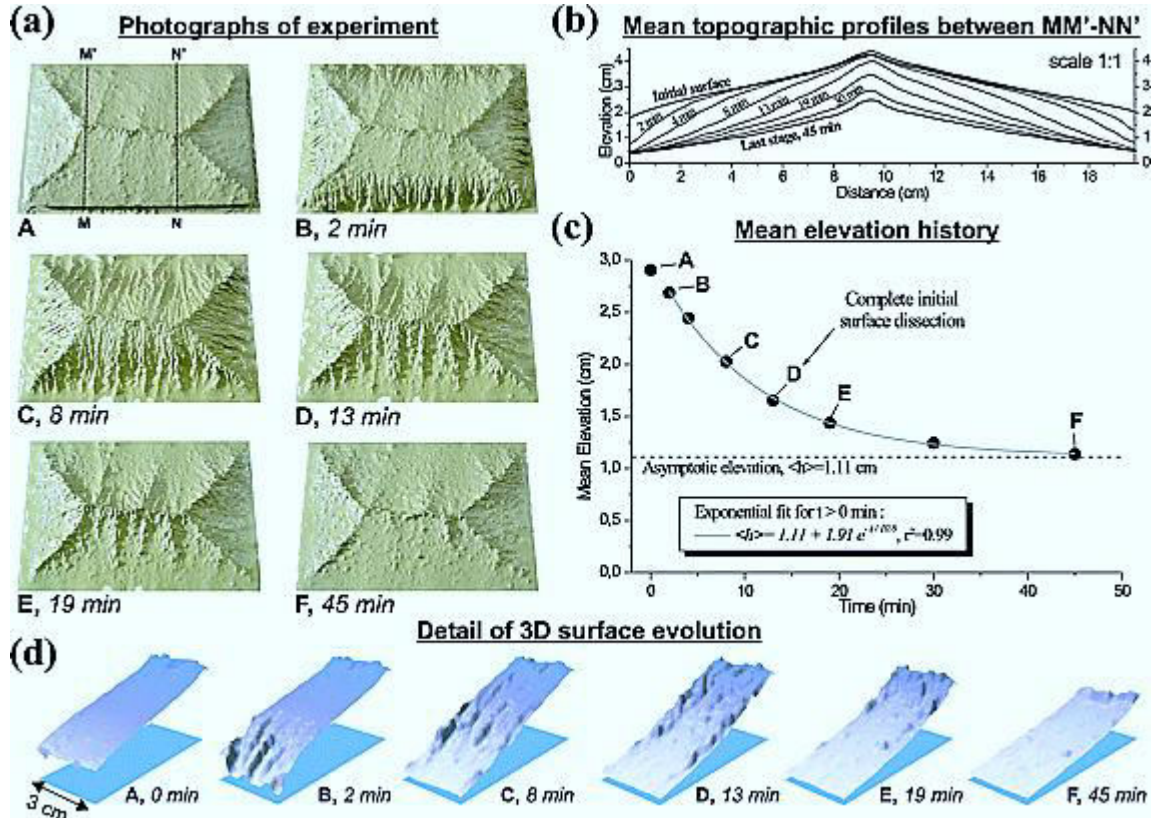

Figure 3.   Relaxation experiment with pre-eroded topography (RE1 experiment).

3.1.2. Organized Initial Topography

[27] In order to test the effect of changing drastically the initial topography, I have reused some previously eroded experiments by raising their surface. The pre-eroded surface makes the connectivity complete even at the initial stage, and the initial drainage network organization in plain view was found to almost keep its initial organization throughout the experimental run (Figure 3a). Compared to the previous experiment, the dynamics of incision growth is qualitatively similar except that the size and spacing of incisions are more uniform, and their propagation is faster Figure 3a). Successive cross-sections (Figure 3b) show that the profile evolution is analogous to random experiments, with an active erosion zone moving inward and widening like a "spreading" wave. Downstream of the active erosion zone, there is no net erosion and the topographic profile tends to its eventual shape. Upstream, there is no erosion either, up to the point when the erosion "wave" reaches the center of the experiment. Then, the crest altitude begins to decrease.

[28] From 2 min until the end of the experiment, the mean elevation decreases exponentially (equation (1)) toward a limit of 1.11 cm, with a response timescale of 10.6 min. As for experiment RR3, the onset

10

of crest erosion, which marks a complete erosion of the experiment surface (stage C), does not correspond to any specific stage of the mean elevation evolution. Note that the topography is eroded on average 3 times faster in these experiments than in RR3, even though the initial average altitude is identical.

3.1.3. Discussion of the Ensemble of Relaxation Experiments: Effect of Initial Topographic Conditions

[29] By changing the initial elevation and initial surface connectivity, My aim to explore the impact of initial conditions on the macroscopic behavior. I mostly concentrate on three main parameters that are described in the previous paragraphs: the characteristic time of the mean elevation decline, the limit elevation, and the characteristic time of connectivity development. The results are synthesized in Table 2 for the six relaxation experiments.
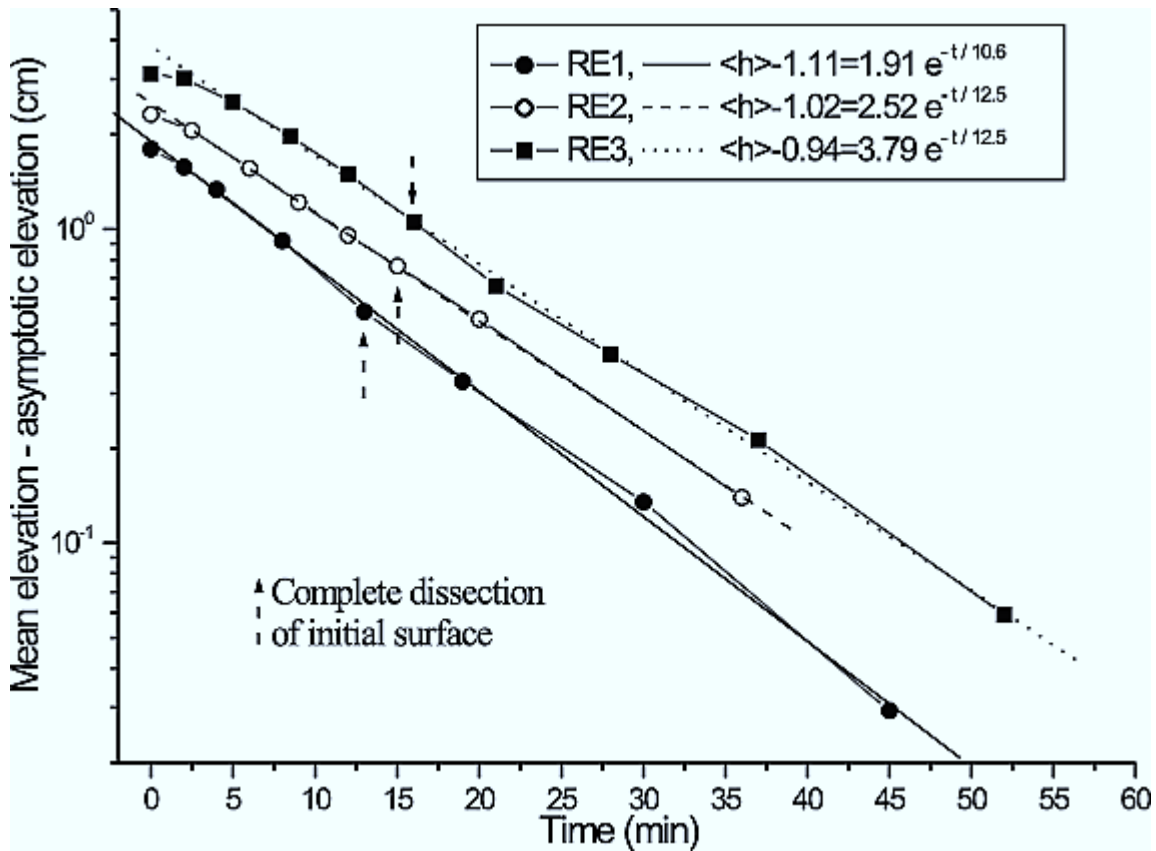

Figure 4. Mean elevation history obtained from experiments of series RE, and exponential fits in semilog diagram. The arrows indicate the connection of opposite incisions. Data represent the mean elevation minus the asymptotic elevation deduced from the exponential fit.

[30] A first remarkable result is that the final height is about 1 cm for all the 6 relaxing experiments whatever the initial topography (height and organization). This limit elevation is likely related to an intrinsic threshold of the erosion law below which no erosion occurs. The limit elevation is thus expected to be independent of initial topographic conditions, while it may obviously depend on the system size or on the drainage organization.
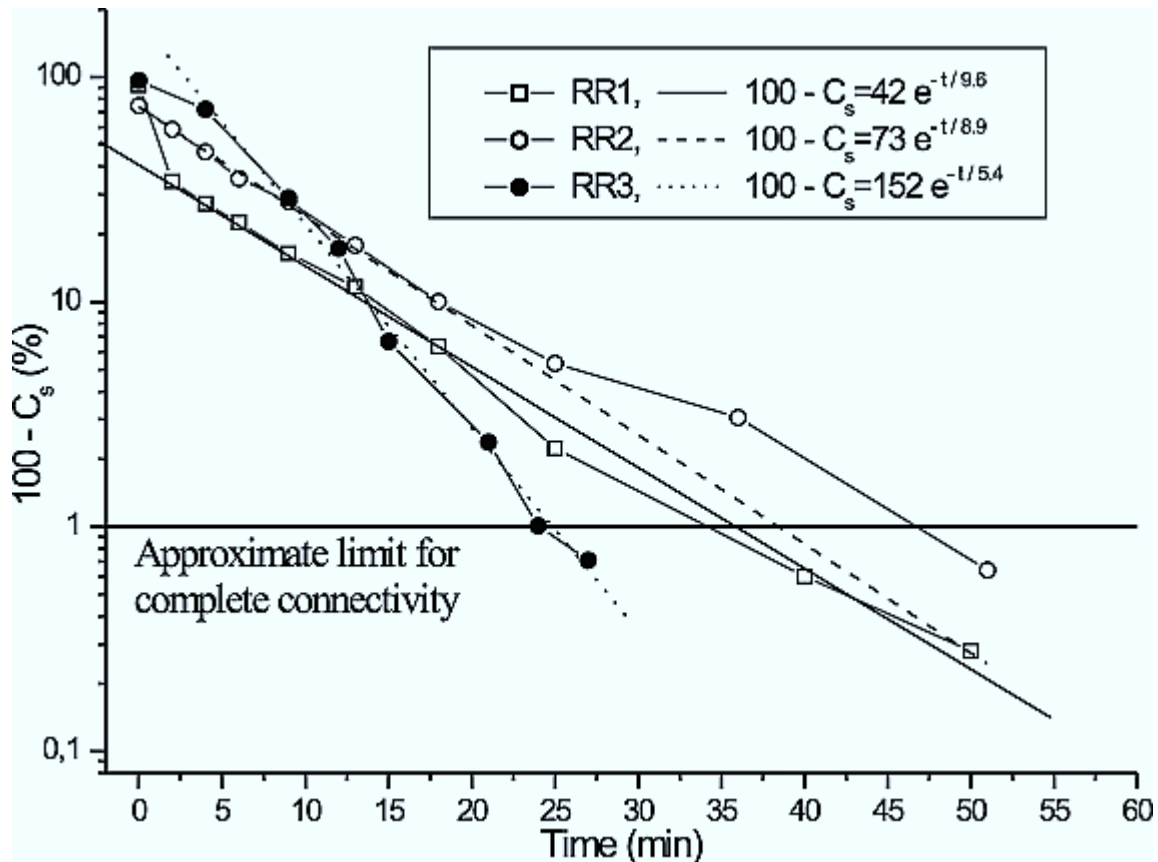
11

Figure 5. Mean elevation history of series RR, and exponential fits in semilog diagram. Data represent the mean elevation minus the asymptotic elevation deduced from the exponential fit. Solid arrows indicate the stage of 99% of connected surface.

[31] For the experiments of the RE series, the characteristic time of the mean elevation exponential decrease (τh in equation (1) and Table 2) is independent of the initial altitude of the pre-eroded surface (Figure 4). In contrast, experiments starting with a random topography (series RR) have a slower evolution, with τ_h of the order of 20 min for experiment RR2 and part of RR3, or 65 min for experiment RR1 and the last stages of RR3 (Figure 5). The difficulty with these random experiments is that most of the erosion (up to 75%) is achieved when the drainage network is being established, that is during the connectivity phase; and the final exponential decrease, if any, is characterized only by a couple of topographic records.

[32] Theoretical studies *[Davy and Crave,* 2000; *Kooi and Beaumont,* 1996; *Whipple,* 2001; *Whipple and Tucker,* 1999] have demonstrated that the characteristic timescale of topographic decline depends on erosion law parameters, system size as well as drainage organization. In particular, when the erosion law depends linearly on slope, the characteristic timescale is independent on initial height. These studies were restricted to erosion laws without a detachment (or transport) threshold; it is however reasonable to suggest that a dependency on initial topographic height reveals a nonlinear dependency of erosion law on slope. The experiments of the RE series address directly this issue since the only variable parameter is the initial elevation. I interpret the fact that the erosion timescale does not depend on initial elevation as an indication of the linearity between erosion rate and slope.

[33] The random experiments give insights into the organization phase of the drainage network. Figure 6 shows that the percentage of surface that remains unconnected to system boundaries decreases roughly exponentially with a timescale τ_c (Table 2) varying between 5.4 and 9.6 min.
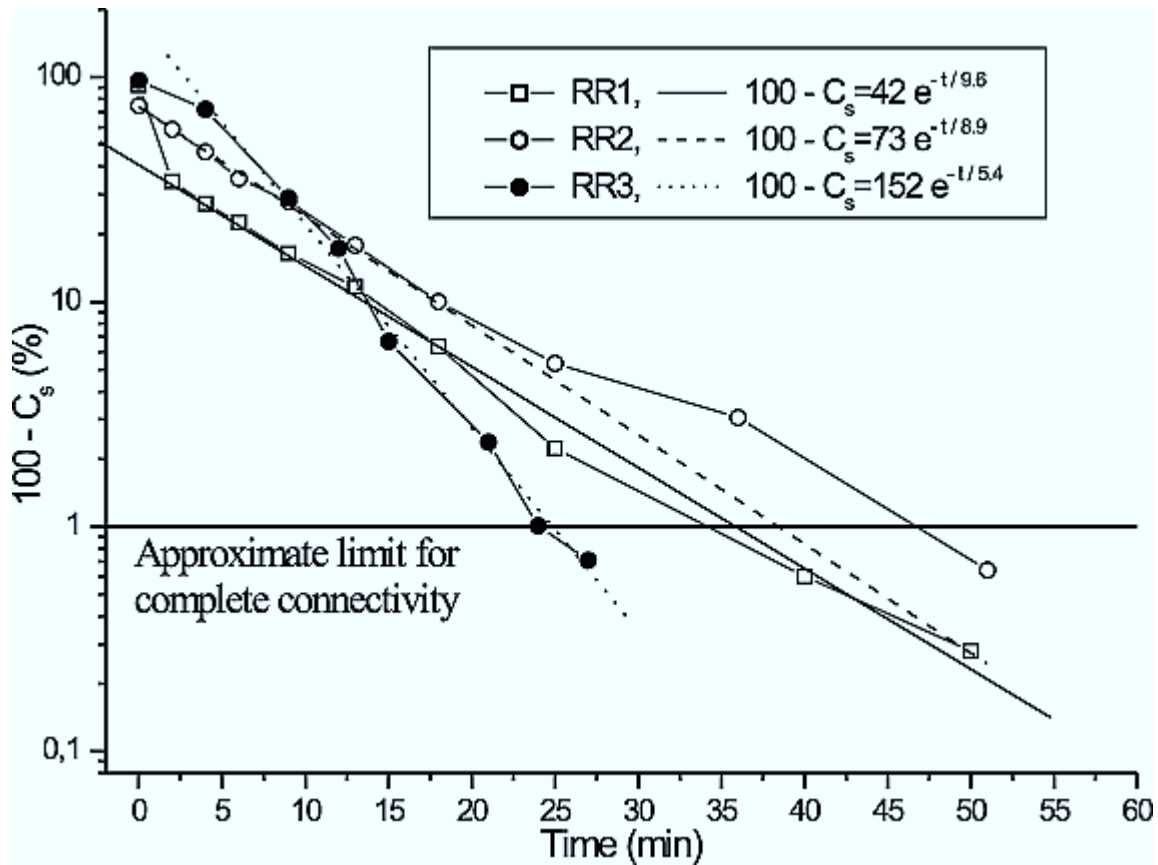
12

Figure 6. Connectivity evolution for RR experiments on a semi-log diagram, and exponential fits. The threshold of connectivity is chosen to be equal to 1% because of small errors in DEM.

3.2. Continuously Uplifted Experiments
3.2.1. Detailed Description of a Typical Experiment

[34] Here I describe in detail one experiment whose initial conditions are a slightly convex plateau with random rugosity, and an uplift rate of 5 cm h^{-1}. Pictures of the surface (Figure 7a) show that small parallel incisions progressively dissect the plateau (stage B), and coalesce forming large and arborescent valley networks (stage C). Unlike the relaxation experiments, continuous uplift maintains large relief near the system boundary and steep topographic profiles (stage D). As further aggregation of elementary incisions occurs, only 3 to 4 main drainage basins remain on each side of the box. These 4-5 cm width basins are finely incised by mm scale rills (stage E-F). After approximately 60 min, the initial plateau is completely dissected and the topography remains constant.

[35] Main topographic profiles taken in the central zone (Figure 7b) illustrate this two-phase evolution: during the first 36 min, the incision zone progressively extends into the uneroded plateau and slopes more and more steeply until reaching a limiting slope of about 25° (Stage D). After 36 min, I observe a small retreat of the topographic profile that becomes weakly, but significantly, concave while the remnants of the plateau are eroded.

There is no clear correlation between τ_c and the initial connectivity or mean elevation. The transitions that are observed in the evolution of the mean elevation (Figure 5) approximately coincide with the completeness of drainage connectivity. This again emphasizes the role of drainage organization on the dynamics of the system.

[36] The mean elevation exhibits also a two-phase history (Figure 7c). Up until 36 min, it increases in accordance with equation (1) with a timescale of about 32 min (see also Figure 9 and its legend). After 36

13

min, the mean elevation becomes suddenly constant at about 3.18 cm. This stage, which is de facto a macroscopic steady state, lasts until the end of the experiment while the topographic profile continues to evolve (Figure 7b). Drainage connectivity increases continuously during the whole evolution in a way that can be fitted by a single exponential function (Figure 7c). The timescale of this exponential increase is
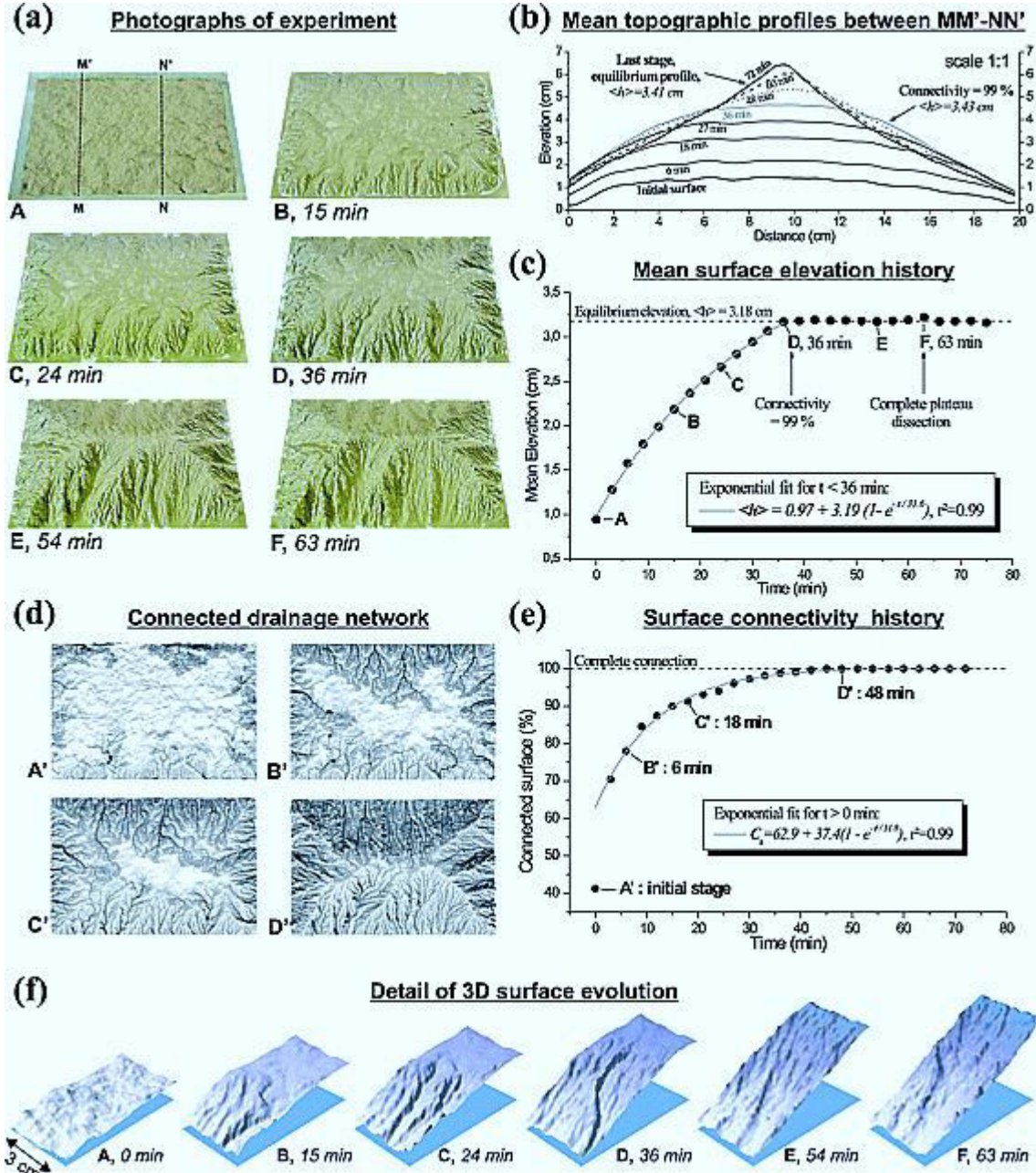

Figure 7. Experiment with uplift and an initial random topography (experiment CR1).

11.8 min. The transition between the two phases observed on the mean elevation evolution occurs for a connectivity of 99%.

[37] At the end of the experiment after about 1 hour, the topography has reached a roughly constant form. The basic organization of the drainage basins remains stable as well as the average topographic shape, which strongly suggests local steady state. Only at the very local scale does one observe very small lateral movements of the fine rill structure.
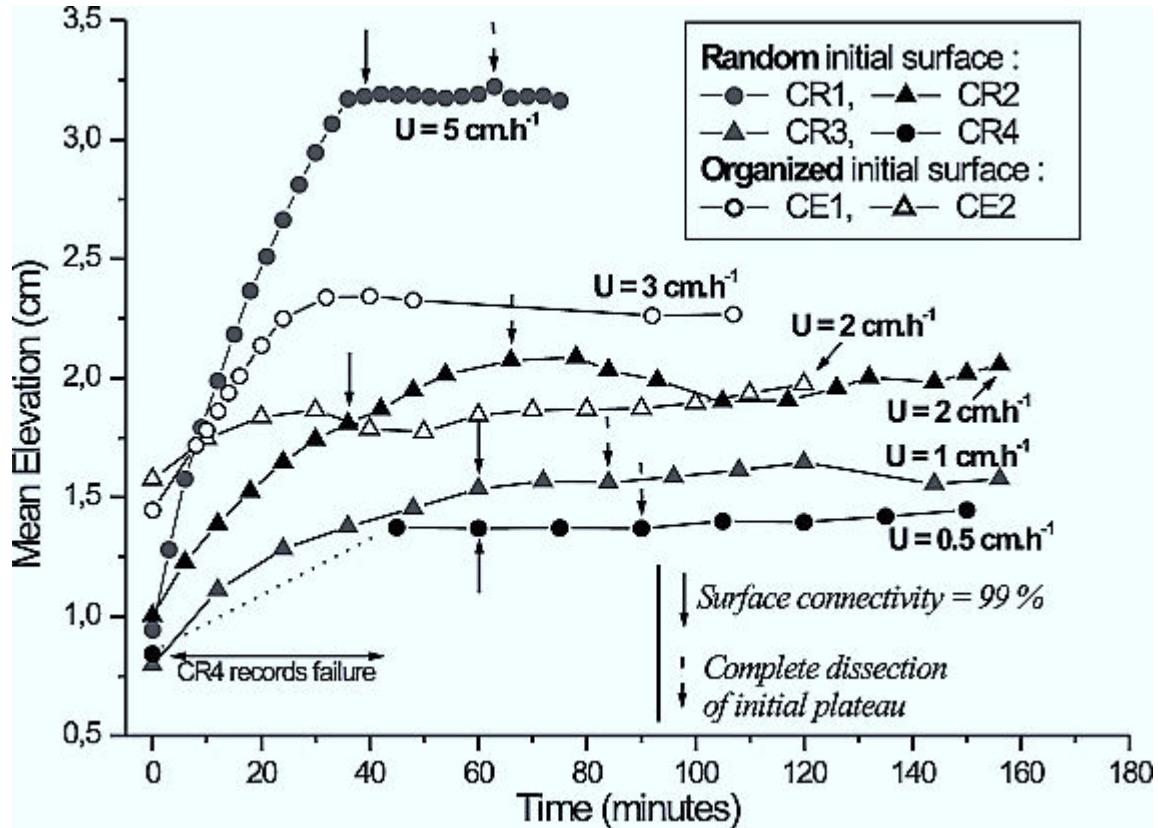
14

Figure 8. Mean elevation history of continuous uplift experiments. A more or less constant elevation is reached after some time. Note that the incisions connect significantly later than the stage of complete drainage network connectivity and the onset of mean elevation stabilization.

3.2.2. Discussion on the Complete Series of Uplifted Experiments

[38] By repeating this experiment with various uplift rates and initial surfaces (Figure 8), the following patterns were observed:

[39] For the CR series (initially random topography), two phases of evolution are systematically observed (Figures 8 and 9). The first phase is adequately modeled by an exponential function (equation (1)). Figure 9 demonstrates the model validity, with a characteristic timescale of about 30 min for all the 3 CR experiments. Figure 9 also shows that a break in the exponential decrease occurs after about 40 -50 min. During this second phase, the mean elevation is about constant but the landscape is still evolving (see in Figure 8 the time when the dissection of the initial plateau ends up). The transition between the two phases coincides with the completeness of drainage connectivity (Figure 9). Note that the steady state phase shows some oscillations of the mean elevation around the long term average (e.g. experiments CR1, CE1 and CR4). This may be due to small variations of the rainfall intensity, something that I have detected when monitoring the rainfall device.

[40] During the growth phase, surface connectivity increases exponentially with characteristic timescales varying between 10.8 and 14.5 min (Figure 10). No systematic correlation between this timescale and the uplift rate is observed.

[41] The CE series is not as well documented for technical reasons. The mean elevation history before equilibrium is well described by the exponential model (equation (1)) for experiment CE2 ($U = 2$ cm h^{-1}, see Figure 8 and Table 2), with a timescale of about 13 min, consistent with the one measured during relaxation experiments. In contrast, the elevation grows rather linearly for experiment CE1 ($U = 3$ cm h^{-1}, see Figure 8), and reaches equilibrium after 20 -30 min. There is no explanation for such difference yet.
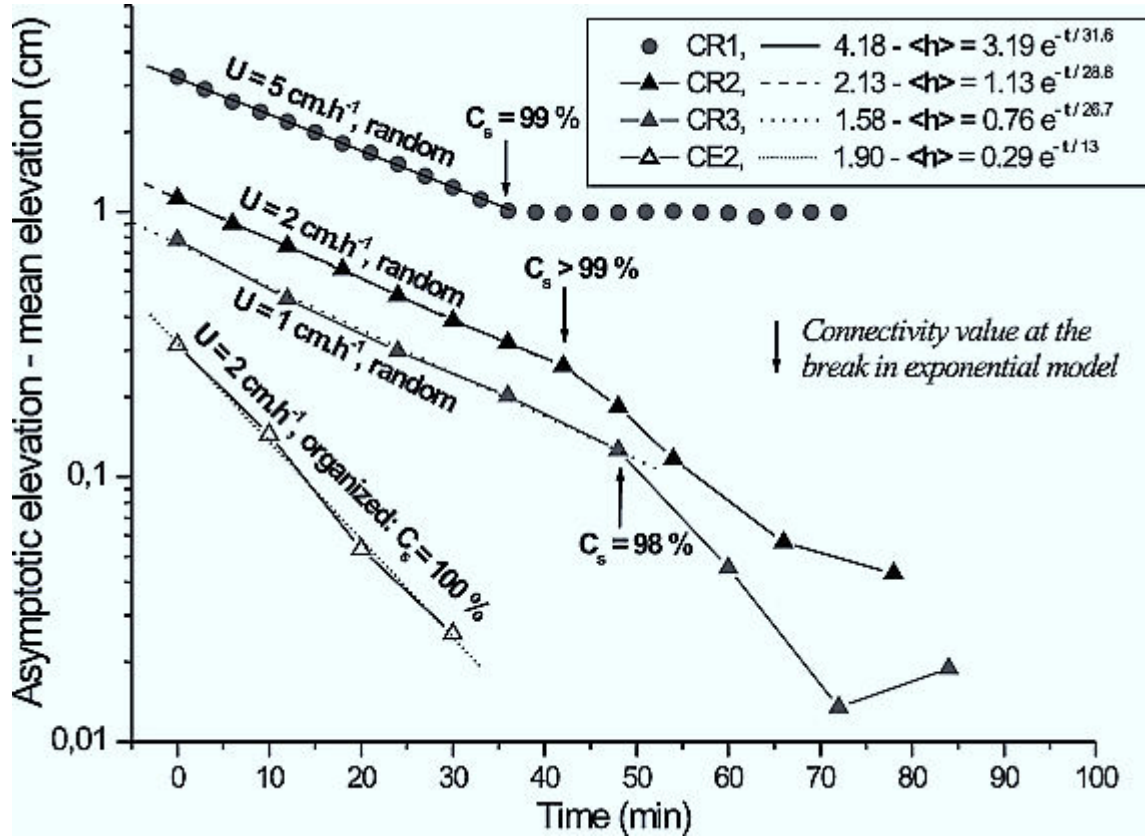
Figure 9. Mean elevation history of CR experiments in a semilog diagram. To underline the exponential behavior, I have ploted the asymptotic elevation minus the mean elevation. Note the shift from exponential decrease to more or less constant elevation in the vicinity of complete connectivity.

3.3. Mean Elevation History

[42] In this paragraph, it is especially focused on the mean elevation history that is on a macroscopic overview of landscape evolution. An interpretation of the topographic organization is presented in the next section.

[43] Whatever the initial conditions, the mean elevation tends toward a constant elevation value which depends on the applied uplift rate. The eventual equilibrium state
corresponds either to a limit elevation for which no erosion occurs that I called a resting state, or to a steady state, also known as dynamic equilibrium *[Hack, 1960]*, for which erosion compensates uplift either on average (macroscopic steady state) or in any place of the system (local-scale steady state).

[44] It was calculated that the mean elevation as the average over the last three stages for all experiments, and was plotted it against uplift rates. A remarkably linear relationship, presented in Figure 11 is obtained:

$$\langle h \rangle_{eq} = \langle h \rangle_u + \tau_u U, \tag{2}$$

with $\langle h \rangle_u$ = 1.19 cm, and τ_u = 23 min. Note that this relationship holds for all experiments whatever the initial surface, demonstrating that the equilibrium stage is independent on initial conditions. The prediction made at $U = 0$ from uplift experiments is roughly consistent with the limit height observed in relaxation experiment.

[45] The timescale τ_u is identical to the timescale τ_h of equation (1) if the average-altitude variation results from a simple

$$d\langle H \rangle / dt = (\langle H \rangle_{\text{limit}} - \langle H \rangle)/\tau \tag{3}$$
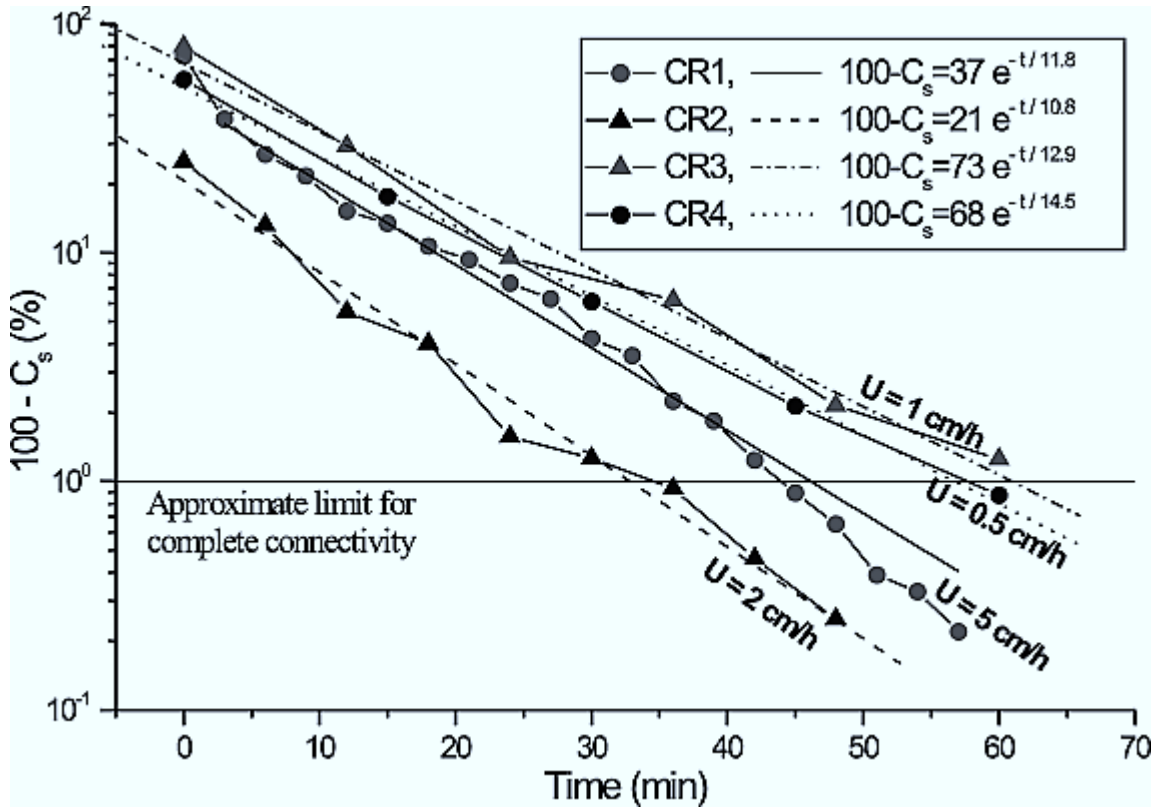
16

Figure 10. Connectivity evolution in a semilog diagram and exponential fits. Note the oscillations around the mean tendency which are caused by incremental capture of puddles of various sizes.
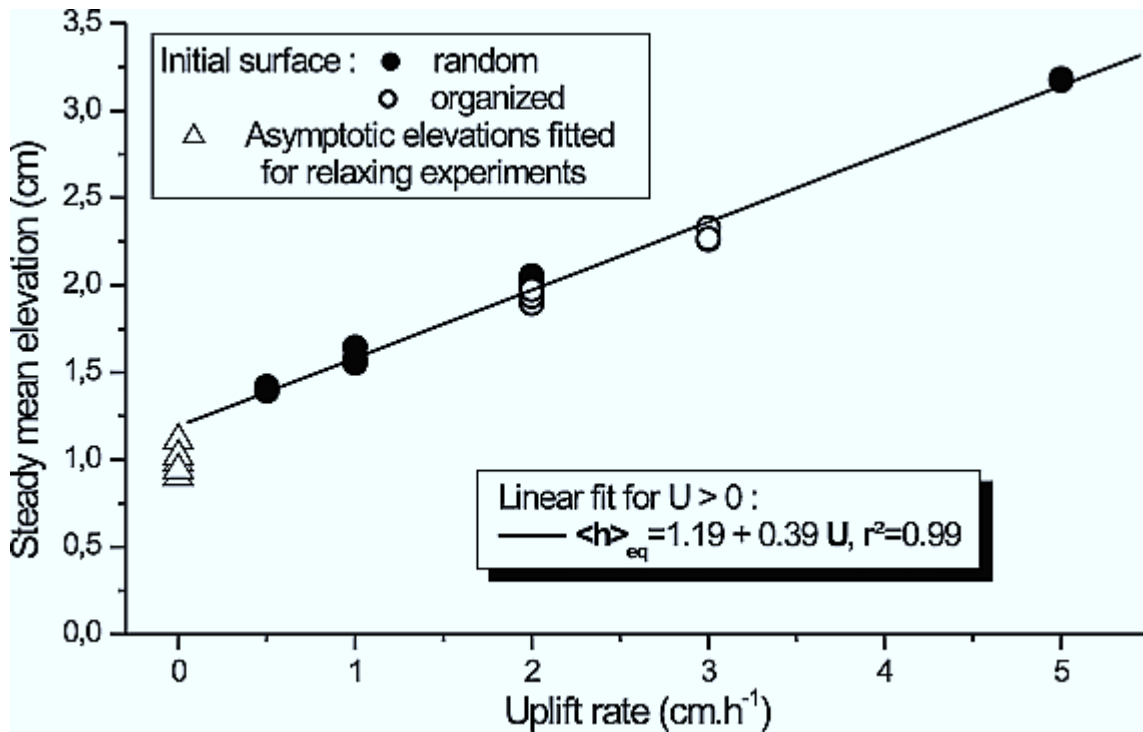

Figure 11. Steady-state mean elevation of the last three stages of continuous uplift experiments starting from various initial surfaces, and asymptotic elevations fitted for relaxing experiments.

for which τ is equal to both τ_h and τ_u Indeed I observe that, for 5 experiments over 10, τ_h is between 20 and 30 min, that is consistent with τ_u considering the difficulty to perform the fit, and especially the uncertainty related to the determination of the height limit. For the four experiments of the CE and RE series—that is with a pre-eroded initial topography—the timescale τ_h is about 10 - 15 min, that is slightly but significantly less than τ_u At last, it remains one experiments of the RR series for which τ_h is 65 min, much larger than τ_u These discrepancies show that the first-order model of equation (3), although not totally inconsistent with experimental results, is too simplistic to account for the whole model dynamics. Evolution of the system connectivity, drainage-network reorganizations, or height variations observed First-order differential equation such as: after the macroscopic equilibrium topographies, render processes that cannot be simply modeled with an equation as simple as equation (3).

4. Analysis of Steady State Topographies

[46] In this section, it was proposed to quantify more precisely erosion-transport processes from steady state topographies. The method used is based on the assumptions that the erosion flux is known in every place at steady state since it exactly compensates the applied uplift, and that the basic parameters of erosion fluxes are local slope and drainage area (a proxy for the local water flow) only, that can be directly quantified from topographic data field. Drainage areas and local steepest slopes were calculated with a flow-routing algorithm from recorded DEM.

4.1. Drainage Organization

[47] The drainage organization is both an outcome and a control of the bulk dynamics. It is quantified by calculating the Hack's law that is the relationship between mainstream length and drainage area for all sub-basins. The Hack's law depends both on the anisotropy of basin shape, and on it's scaling with basin area.

[48] For all experiments, it was found that Hack's law is not significantly dependent on uplift rate (Figure 12), and on initial surface conditions. For areas smaller than 10 mm^2, the mainstream length increases almost linearly with drainage area, indicating that flow lines are roughly parallel. For larger areas, the mainstream length increases as the square root of the drainage area indicating a tree-like convergent structure of the flow. The Hack exponent is in the range of values computed for natural basins *[Rigon et al., 1996]*. The independence of the drainage organization with uplift has already been recognized in natural systems *[Hurtrez et al., 1999]*, and demonstrates that the mechanisms that make the drainage-network organization are independent of bulk erosion intensity, and in particular of sediment concentration.

4.2. Slope-Area Relationships

[49] It is calculated that the mean area-slope relationship for the three last surfaces of each uplift experiments (Figure 13). the first observation is that, for drainage areas greater than $1\,\text{mm}^2$ and for uplift rates ranging between 0 and 3 cm h^{-1}, the mean local slope decreases with drainage area according to a power law relationship:

$$S = kA^{-\theta} \tag{4}$$

where k is called the steepness index and θ the area-slope exponent or concavity index *[Snyder et al., 2000]*. This power law relationship is valid for drainage areas larger than $1\,\text{mm}^2$, suggesting that there is only one erosion mechanism that shapes topography across all scales. There is no indication of diffusive processes such as rain splash erosion, since the gradients of the area-slope relationship are always negative *[Willgoose et al., 1991a]*. For an uplift rate of 5 cm h^{-1}, the slope -area relationship is no more a power law although a power law fit yields parameters k and θ consistent with lower uplift rates experiments (Figure 13).

[50] Careful analysis of θ and k, shows: (i) that θ is equal to 0.12 ± 0.01 whatever the uplift rate and the initial surface conditions (Figure 14), (ii) that for strictly positive uplift rates, k is proportional to uplift

18

rate (Figure 14):

$$k = 0.334 + 0.0158\,U, \qquad\qquad (5)$$

where U is in mm h^{-1} and k is in mm$^{0.24}$.

[51] Relaxation experiments are about consistent with uplifted ones, with a steepness index that either fits equation (5), or is slightly smaller than the value predicted at $U = 0$. Given that the relaxation stages considered may be not completely at resting state (the observed value of $\langle h \rangle_{\text{limit}}$ is larger than the one predicted by an exponential decrease, Table 2), a steepness index of 0.22-0.25 is more likely for relaxation experiments, as calculated for experiment RR3 for which the relaxation steady state is effect power law relationship: timely reached (Figure 5). There is no significant difference in the area-slope exponent 9 between uplifted and relaxation experiments.
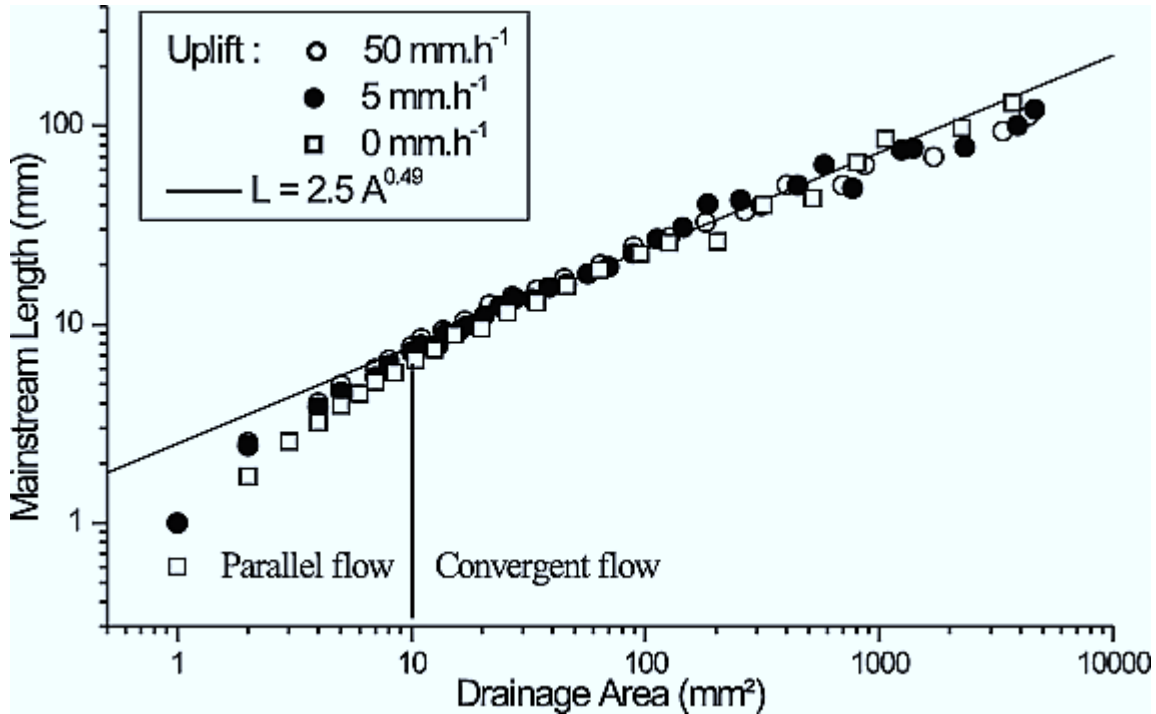

Figure 12. Mainstream length evolution in function of drainage area for three experimental basins (CR1, CR4 and RR3).

[52] Given that the drainage network organization is independent of uplift rate (Figure 12), local topography responds to uplift by changing its local slope according to upstream area and uplift rate. The fact that for uplift rates ranging between 0 and 3 cm h^{-1} the area-slope relationship is a power law, and that the power law exponent is independent of scale and of uplift rate (Figure 14), strongly indicates that the steady state topographies are shaped by a single erosion-transport process. In contrast the deviation from the power law model that is observed for experiment at 5 c m h^{-1} may underline a change in the nature of the erosion-transport process due to higher sediment concentration ($C_v \sim 50\%$ for $U = 5$ cm h^{-1}, compared to $C_v \sim 30\%$ for $U = 3$ cm h^{-1}): erosion processes might shift from runoff erosion to erosion by mud slurries
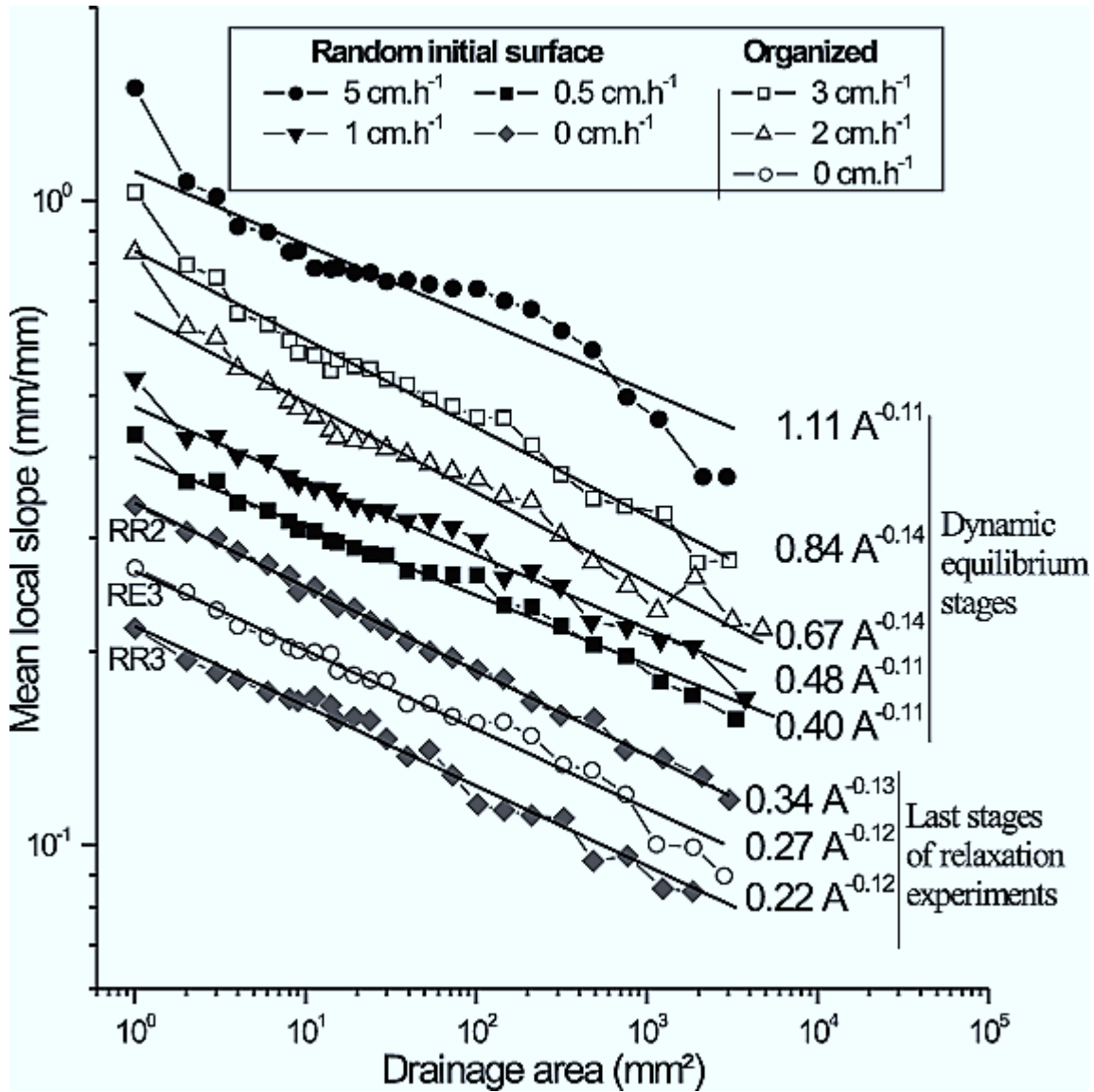
Figure 13. Area-slope relationships for the last recorded surface of some CR, CE, RE and RR experiments. The data points represent the logarithm bin of raw data for the entire surface.

4.3. Theoretical Interpretation
4.3.1. Stream Power Law Model
[53] On the previous elaborated results in defining a set of equations that quantifies the sediment transport processes at dynamic equilibrium. In the following, it is assumed that topography has reached a complete local steady state, i.e. in each point of the system, erosion totally balances uplift. To understand the previous results, it is required to know precisely the sediment transport mode, in particular the average travel distance of a particle once it has been detached. Since there is no access yet to this characteristic, there is no unique solution for the erosion model (cf. paragraph 1.2 *[Tucker and Whipple, 2002; Whipple and Tucker, 2002]*). Thus
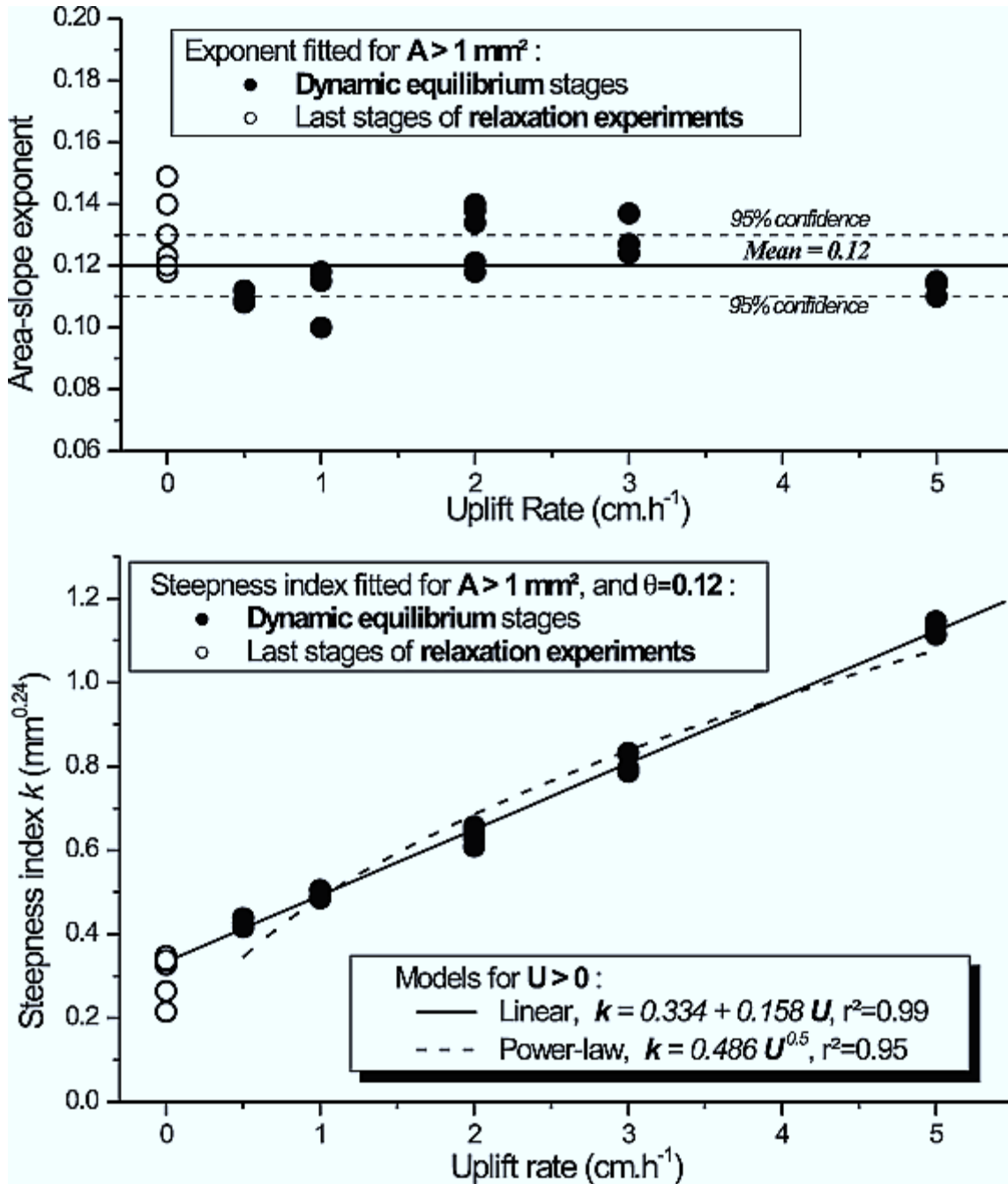
20

Figure 14. Area-slope exponent 9 and steepness index k derived by fitting data with an area-slope model: $s = kA^{-\theta}$ explore two end-member models: the first which considers that the particle travel distance is short, or that the particle fall velocity is smaller than flow velocity (bed load transport belongs to this category that is generally called transport-limited model), and the second which considers that the flow can transport a particle over long distances once detached (equivalent to suspended load transport and generally called detachment-limited model). In the former case (transport-limited), the sediment flux is always equal to the sediment transport capacity Q_c. At steady state, given that the sediment flux is equal to the upstream volume of sediment uplifted per time at any point of the topography, thus have:

$$Q_c = UA \tag{6}$$

In the detachment-limited case, detachment rate E (incision rate) is simply equal to uplift rate:

$$E = U. \tag{7}$$

[54] Defining the expressions for Q_c and E in terms of the physical variables of flow is a key issue in geomorphology. The most commonly used formula is the stream-power law, where the sediment transport capacity or the detachment rate is a function of the water discharge Q_w, to a power m, and of the topographic gradient S to another power n. m and n are exponents that control the topography dynamics and shapes *[Davy and Crave, 2000; Howard, 1994; Tucker and Bras, 1998; Tucker and Whipple, 2002; Whipple and Tucker, 1999, 2002]*. The stream power law model is widely used in geo-morphological studies *[Howard et al., 1994; Kirkby, 1971; Lague et al. , 2000; Smith and Bretherton, 1972; Tarboton et al., 1992; Whipple and Tucker, 1999; Willgoose etal., 1991a]*, as well as in soil erosion studies *[Govers, 1992b; Hairsine and Rose, 1992]*. Several writers have discussed the importance of a detachment (resp. transport) threshold in the stream power law model *[Densmore et al., 1998; Howard, 1980, 1994; Howard and Kerby, 1983; Snyder et al., 2002; Tucker and Bras, 1998, 2000; Tucker et al., 2001; Tucker and Slingerland, 1997]*. In this experiments, the existence of a remaining elevation in relaxation experiments demonstrates that a particle detachment threshold have to be incorporated into the stream power law expression. Thus use the following expressions for the transport-limited and detachment-limited models respectively:

$$\left. \begin{aligned} &if Q_w^m S^n \leq \xi_Q, \text{then } Q_s = 0 \\ &if Q_w^m S^n \leq \xi_Q, \text{then } Q_s = k_s \left(Q_w^m S^n - \xi_Q \right)^r \end{aligned} \right\} \tag{8a}$$

and

$$\left. \begin{aligned} &if Q_{w'}^{m'} S^{n'} \leq \xi_E, \text{then } E = 0 \\ &if Q_{w'}^{m'} S^{n'} \leq \xi_E, \text{then } Q_s = k_s (Q_{w'}^{m'} S^{n'} - \xi_E)^{r'} \end{aligned} \right\} \tag{8b}$$

for the sediment flux and detachment rate respectively. In the above equations, k_s and k_e are transport and detachment coefficients respectively, which includes the effect of material cohesion, material density and channel geometry, ξ_Q and ξ_E are thresholds whose dependency with slope and water flux is yet unknown and m, n, r , m', n', r' are exponents. Since the rainfall is steady and roughly uniform, the water discharge Q_w is equal to the product of drainage area by precipitation rate. Introducing equations (6) and (7) in equation (8) gives:

$$k_s \left(p^m A^m S^n - \xi_Q \right)^r = UA, \tag{9a}$$

and

$$k_e (p^{m'} A^{m'} S^{n'} - \xi_E)^{r'} = U, \tag{9b}$$

which gives the following expressions for the slope–area relationship *[Howard, 1994; Tucker and Bras, 1998]*, in the transport-limited and detachment-limited cases respectively:

$$S = \left(p^{-m} \xi_Q + p^{-m} \left(\frac{U}{k_s} A \right)^{1/r} \right)^{1/n} A^{\frac{m}{n}}, \tag{10a}$$

and

$$S = \left(p^{-m'} \xi_E + p^{-m'} \left(\frac{U}{k_e} \right)^{1/r'} \right)^{1/n'} A^{\frac{m'}{n'}} \tag{10b}$$

Equations (10a) and (10b) predict a relationship between slope, drainage area and uplift rate consistent with the experimental one:

$$S = (a + bU)A^{-\theta}, \tag{11}$$

where $\theta = 0.12$, $a = 0.334$ mm$^{0.24}$ and $b = 0.0158$ mm$^{-0.76}$ h (equations (4) and (5)). For the transport limited model equation (11) implies that n and r are unity, and that ξ_Q is proportional to drainage area: $\xi_Q = k_\xi A$, with k_ξ a constant. Thus, equation (10a) becomes:

$$S = \left(p^{-m}k_\xi + \frac{p^{-m}}{k_s}U\right)A^{\frac{m-1}{n}} \tag{12}$$

[55] By identifying corresponding terms between equations (11) and (12), and equations (11) and (10b), I obtain the following expressions of the sediment transport capacity Q_c, and of the detachment rate E for the transport-limited and detachment-limited models respectively:

$$Q_c = \frac{1}{b}(A^{1.12}S - aA), \tag{13a}$$

$$E = \frac{1}{b}(A^{0.12}S - a), \tag{13b}$$

The values of the transport capacity and incision laws parameters (equation (8)) are deduced from equation (13), knowing that p = 100 mm h^{-1}: $m = 1.12$, $n = 1$, $r = 1$, $k_s = 63.3$ mm$^{-0.36}$ h$^{0.12}$, $k_\xi = 0.334$ mm$^{1.36}$ h$^{-1.12}$, $m' = 0.12$, $n' = 1$, $r' = 1$, $k_e = 63.3$ mm$^{0.64}$ h$^{-0.88}$ and $\xi_E = 0.334$ mm$^{0.36}$ h$^{-0.12}$. For both equations, sediment fluxes depend linearly on slope. Note that fitting a power law relationship (i.e., erroneously assuming that the threshold is negligible) to the steepness index relationship (Figure 14) gives very different exponents of $n = 2$ and $m = 1.24$ for the transport-limited model, and of $n' = 2$, $m' = 0.24$ for the detachment-limited model. precipitation rate. Introducing equations (6) and (7) in equation (8) gives:

4.3.2. Critical Shear Stress for Incipient Motion
[56] For relaxation experiments, the resting surface is such that the basal shear stress is equal to the critical shear
stress of particle detachment τ_{cr} everywhere on the surface. Assuming a steady laminar flow, and a power law relationship between flow width and drainage area $w = \beta A^a$, a theoretical derivation of the area-slope relationship would give (Appendix A)

$$S = \frac{\tau_{cr}^{3/2}}{g\rho_w^{3/2}}\left(\frac{8\beta}{pk_rv}\right)^{1/2} A^{\frac{1-0}{2}},$$

where k_r is a dimensionless roughness factor (of the order of 40). Given that the slope-area exponent is 0.12, this expression predicts an area-width exponent a of 0.76, significantly higher than the empirical exponent of 0.5 obtained for natural [Leopold and Maddock, 1953] and experimental alluvial rivers [Schumm et al., 1987], or measured in bedrock river (0.3-0.5 [Montgomery and Gran, 2001]; 0.3-0.4 [Snyder et al., 2002]).
[57] τ_{cr} is then determined from the steepness index of relaxing topographies at resting state, k_o:

$$\tau_{cr} = \left(k_0^2 \frac{pkvg^2\rho_w^3}{8}\right)^{1/3}\beta^{-\frac{1}{3}},$$

or $\tau_{cr} \approx 2.6\beta^{-1/3}$, for $k_o = 0.22$ mm$^{0.24}$. Assuming that 3 varies between 1 and 10 m$^{-0.5}$ (in order to obtain realistic values of channel width), the corresponding critical shear stress varies between 1.2 and 2.6 Pa, in the range of estimated values for fine-grained soil erosion [Govers, 1992a; Torri et al., 1987].

4.3.3. Mean Elevation-Uplift Rate Relationship

[58] I can now easily bridge the gap between the slope -area relationship and the linear relationship between mean elevation at steady state and uplift rate. By using the slope-area relationship and Hack's law, I can calculate the form of a profile of the topography as a function of uplift rate *[Whipple and Tucker,* 1999]. Integrating the slope from the crest *(x* = 0) gives the elevation at any point of the stream profile:

$$h(x) = - \int_0^x (a + bU)\, A(x)^{-\theta} dx + h(0)$$

where $a = 0.334$, $b = 0.0158$ and $\theta = 0.12$, and $A(x)$ is given by Hack's law $A(x) = x^2/c$. Given that $1 - 2\theta \neq 1$, $h(x)$ can be integrated over x to give:

$$h(x) = h(0) - \frac{(a+bU)}{(1-2\theta)c^{-2\theta}} x^{1-2\theta} \tag{14}$$

If L is the total profile length, I can derive the basin relief that is the elevation difference between crest and outlet:

$$h(0) - h(L) = \frac{L^{1-2\theta}}{(1-2\theta)c^{-2\theta}} (a + bU). \tag{15}$$

The relief is shown to be proportional to uplift, and to keep a strictly positive value in relaxation experiments *(U =0)*. The mean profile elevation is:

$$\langle h \rangle_p = \frac{1}{L} \int_0^L h(x)\, dx.$$

By using equations (14) and (15), $\langle h \rangle_p$

$$\langle h \rangle_p - h(L) = \frac{(a + bU)}{L(1 + 2\theta)c^{-2\theta}} \int_0^L \left(L^{1-2\theta} - x^{1-2\theta} \right) dx$$

$$= \frac{L^{1-2\theta}}{(2 - 2\theta)} c^{-2\theta} (a + bU). \tag{16}$$

[59] Note that, although difficult analytically, it is technically possible to integrate over the complete basin in order to estimate its mean elevation. By comparison to $\langle h \rangle_p$, the mean basin elevation would have a different scaling with $L,$ but a similar linear dependency with the uplift rate $U.$ The latter comes from the linear relationship between sediment flux (resp. detachment rate) and local slope *(n* = 1, equations (8) and (13)).

[60] Equation (16) gives thus a rationale to equation (2), and to the parameters $\langle h \rangle_u$ and τ_u, which are the remaining elevation in the absence of uplift and a characteristic time-scale, respectively. Considering the theoretical expression of *a* and *b* given by using equations (14) and (15), $\langle h \rangle_p$ becomes: equation (2), it is found that equation (16) predicts that both τu and $\langle h \rangle u$ would increase (i) by increasing system size, (ii) by decreasing precipitation rate, and (iii) by decreasing erosion transport efficiency k_s (k_e resp.). Note however that the characteristic timescale is independent of the detachment (resp. transport) threshold.

5. Discussion

5.1. Comparison with Surface Process Modeling Predictions

[61] Given that runoff erosion in these experiments can be modeled by a stream power law, the set of experiments provides a physical framework for testing important outcomes of surface process models, in particular of theoretical works based on this stream-power formulation of erosion-transport processes. In contrast to geometries at steady state that can be derived analytically *[Tucker and Whipple,* 2002; *Whipple and Tucker,* 2002; *Willgoose et al.,* 1991a], the transient dynamics remain a key issue for which experiment dynamics, even if not perfectly analogous to natural systems, may provide some interesting information. For instance, experiments confirm that in the case of stable and connected drainage network, and of detachment rate proportional to local slope, the mean elevation evolves exponentially with time, with a characteristic timescale independent of initial uplift step, and of uplift rate *[Davy and Crave,* 2000; *Kooi and Beaumont,* 1996; *Whipple,* 2001; *Whipple and Tucker,* 1999]. It also demonstrates that surface connectivity plays a key role in system dynamics, a finding which agrees with observations that drainage capture due to an initially unconnected part of the topography strongly affects the sediment flux history *[Kooi and Beaumont,* 1996; *Tucker and Slingerland,* 1996]. Even if I do not explicitly demonstrate it, the existence of a nonnegli-gible threshold is likely to play a critical role in the response time of the evolution of connectivity.

[62] As observed by *Hasbargen and Paola* [2000] during longer steady state experiments, drainage network and topography can vary during dynamic equilibrium, unlike numerical modeling predictions. However, I believe that
these variations partly originate from time and spatial variations in rainfall intensity that may reach 20% over 5 min. I currently working on a better rainfall generator in order to test this hypothesis.

5.2. Detachment- or Transport-Limited Processes

[63] As discussed in a previous section, the form of the final topography does not quantify unambiguously the erosion process *[Whipple and Tucker,* 2002]. An important issue is the mode of sediment transport in the system with at least two end-members that have already been described: detachment-limited and transport-limited models. Erosion models in which detachment rate is a function of sediment load *[Sklar and Dietrich,* 1998, 2001] could also explain the area-slope relationships at steady state *[Whipple and Tucker,* 2002]. However, this type of process is unlikely to be important or even operative in the experiments.

[64] A surface process model is used *[Crave and Davy,* 2001; *Davy and Crave,* 2000] which reproduces the mechanisms of sediment detachment and transport on a 2D surface to explore the transient dynamics of each possible transport mode. The detachment model obeys the same equations than I find for experiment that is a stream power law with a threshold (equation (13). In this numerical model, the deposition flux is proportional to the sediment concentration, so that in the absence of erosion, the quantity of deposited sediment varies exponentially along stream with a characteristic length scale L_t that represents a typical sediment transfer distance *[Beaumont et al.,* 1992]. If L_t is small, the topography dynamics is similar to a transport-limited model for which the rate of elevation change varies as the gradient of erosion flux. If L_t is very large, the sediment can leave the system without being redeposited, as for an erosion-limited model. Details of the numerical implementation are available in the work of *Crave and Davy* [2001].

[65] For the sake of simplicity, I have used the initial surface of the RE1 experiment as an initial condition of the simulations with a pixel size of 1 x 1 mm focus. For this experiment, the drainage network is already connected at the initial stage, and its planar organization remains roughly stable. Figures 15a and 16a show the mean average topographic profile evolution and DEM, respectively, of the reference experiment RE1. Figures 15b, 15c, 15d and 16b, 16c, 16d show simulations performed for three different values of L_t, that is 1 mm, 200 mm and 10,000 mm. These values should be compared with the system size which is 200 mm.
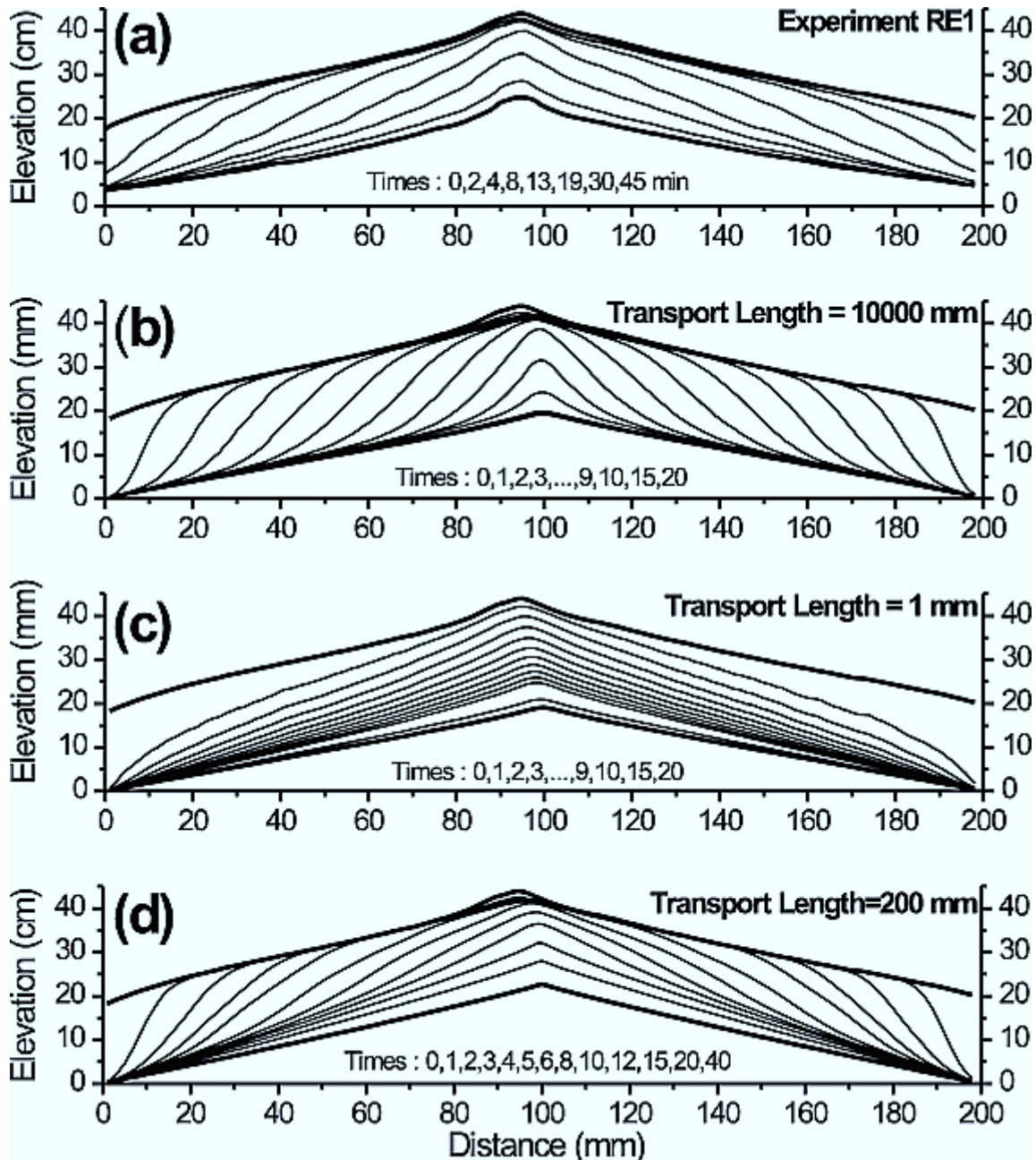
Figure 15. Mean topographic profiles of the central part (7 cm-wide SWATH profiles as in Figure 3) of experiment RE1 (a), and of numerical simulations presented in the text (b, c and d). The sediment transfer length L_t is 10,000 mm (b), 1 mm (c) and 200 mm (d) respectively.

[66] If L is large (detachment-limited model, Figure 15b), erosion proceeds by an inward retreat of the initial surface from the boundary conditions. The active erosion zone is much more localized than in experiments of series RE. In contrast, if L_t is small (transport-limited model, Figure 15c), erosion is spatially diffuse and affects the whole domain even at the earliest stages. Note that both models give the same topography at resting state.

[67] A good agreement with experimental results is obtained when L_T is of the order of the system size (Figure 15d), with both a retreat of the initial plateau and a diffusive widening of the active erosion zone. Under this formalism, the average sediment transport length of particles is about the system size, so that erosion mechanisms varies from detachment-limited upstream to transport-limited downstream near the outlet. This preliminary calibration of erosion process is open to more refinement, but the good agreement

between the transient dynamic of experiments and simulations shows that the stream power law model, including detachment threshold, and the sediment transport length are basic ingredients to fully understand experiment dynamics. Currently it is undertaken experiments in a flume to address the issue of the sediment transport mode, and of the transport length concept more specifically.

5.3. Analogy with Natural Systems
5.3.1. Formal Analogy
[68] The experiments reproduce several features of natural systems: (1) topography evolves by the growth of incisions which spontaneously organize into a drainage network whose steady state geometry is similar to natural systems (Hack exponent ≈ 0.5); (2) the steady state topographies are characterized by a well-defined area-slope relationship with a negative power law relationship between slope and drainage area that is characteristic of unstable surface with respect to erosion instabilities *[Smith and Bretherton,* 1972; *Tarbo-ton et al.,* 1992]; (3) as for a large number of natural processes (alluvial channels *[Howard,* 1980; *Talling,* 2000]; hillslope gullying *[Vandaele et al.,* 1996]; bedrock incision *[Lave and Avouac,* 2001; *Snyder et al.,* 2002]), particle detachment (resp. transport) requires a threshold to be overcome before significant erosion and transport occurs.

[69] But the analogy is obviously incomplete. There is only one single erosion process—in the sense of a stream power law process—in experiments while natural watersheds often exhibit several erosion-transport regimes. Water
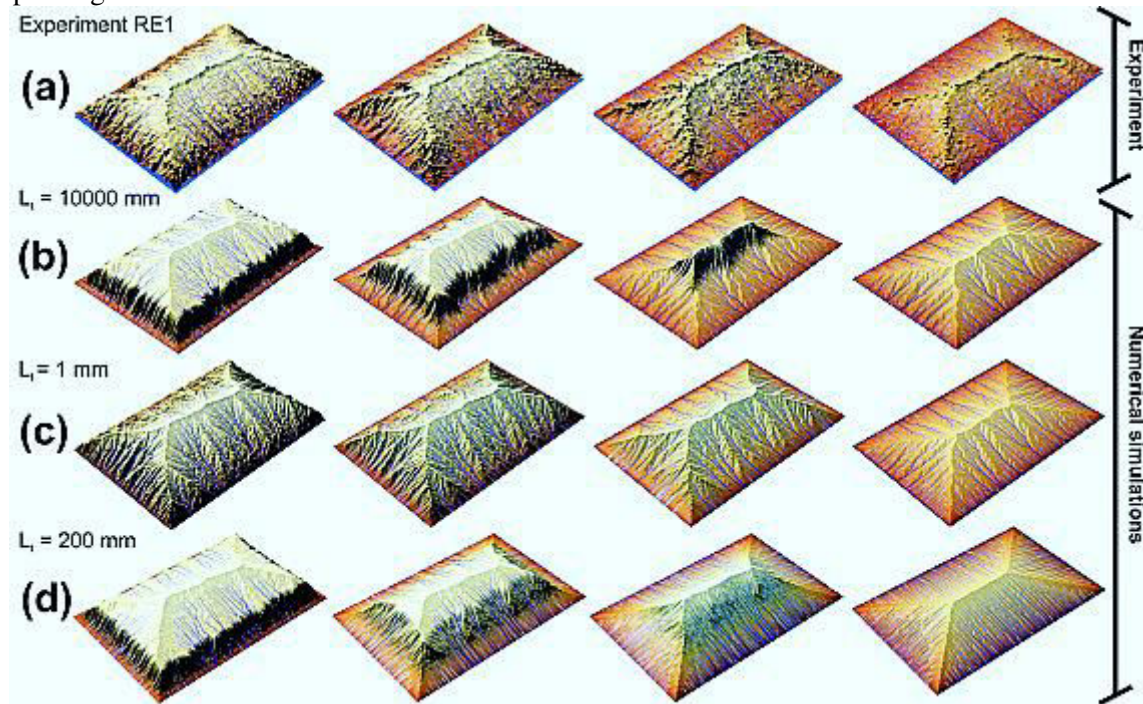

Figure 16. DEM of the experiment RE1, and of numerical simulations. The simulation parameters are in the text. The presentation is similar to Figure 15.

flow is by far too laminar and sediment concentration is often too high to represent a correct analog of river channels *[Hasbargen and Paola,* 2000]. This is consistent with the slope -area scaling exponent θ, which is supposed to characterize the erosion mechanism *[Tucker and Bras,* 1998], and which is significantly lower than the range of value measured in bedrock and coarse-grained alluvial rivers ($\theta \approx$ 0.4-0.7, sometimes greater than 1 *[Flint,* 1974; *Hack,* 1957; *Ijjasz-Vasquez and Bras,* 1995; *Lague et al.,* 2000; *Montgomery and Foufoula-Georgiou,* 1993; *Seidl and Dietrich,* 1992; *Snyder et al.,* 2000; *Whipple and Tucker,* 1999, 2002; *Willgoose etal.,* 1991a]; see also *Tucker and Whipple* [2002] for a review). Slope-area exponents lower than 0.25 were obtained in three different cases: (i) for random gaussian

surfaces [*Schorghofer and Rothman,* 2001, 2002], (ii) in badlands alluvial channels, ephemeral gullies and finegrained alluvial rivers ($\theta \approx$ 0.11-0.24 [*Howard,* 1980; *Howard and Kerby,* 1983]), and (iii) in debris-flow dominated colluvial channels ($\theta \approx$ 0.15 estimated from *Montgomery and Foufoula-Georgiou* [1993] and *Snyder et al.* [2000]), although in that latter case the stream-power law model has not yet a physical support, and is even questionable with respect to field data (J. Stock and W. E. Dietrich, Valley incision by debris flows: Evidence of a topographic signature, submitted to *Water Resources Research,* 2002). Even if likely, the null-hypothesis of a random signature to explain such low slope -area exponents [*Schorghofer and Rothman,* 2001, 2002] cannot account for long range correlation that makes the flow network entirely connected to boundaries. I prefer thinking that it reveals a physically sound erosion process. Experiments are likely to be analog of fine-grained alluvial rivers if I consider only the nature of the eroded material. However, I do find striking analogy with steep colluvial valleys in mountainous area. An example is given in Figure 17 that shows a comparison between an experiment and a small basin of the Pachmarhis (Central India), where steep colluvial valleys are observed, and where topography is likely to be in steady state. The power law relationship $S \propto A^{-0.14}$ is valid between $8 \ 10^{-3}$ and $\sim 1 \, \mathrm{km}^2$, and is similar to any experimental curve, except of course the difference in area scales.
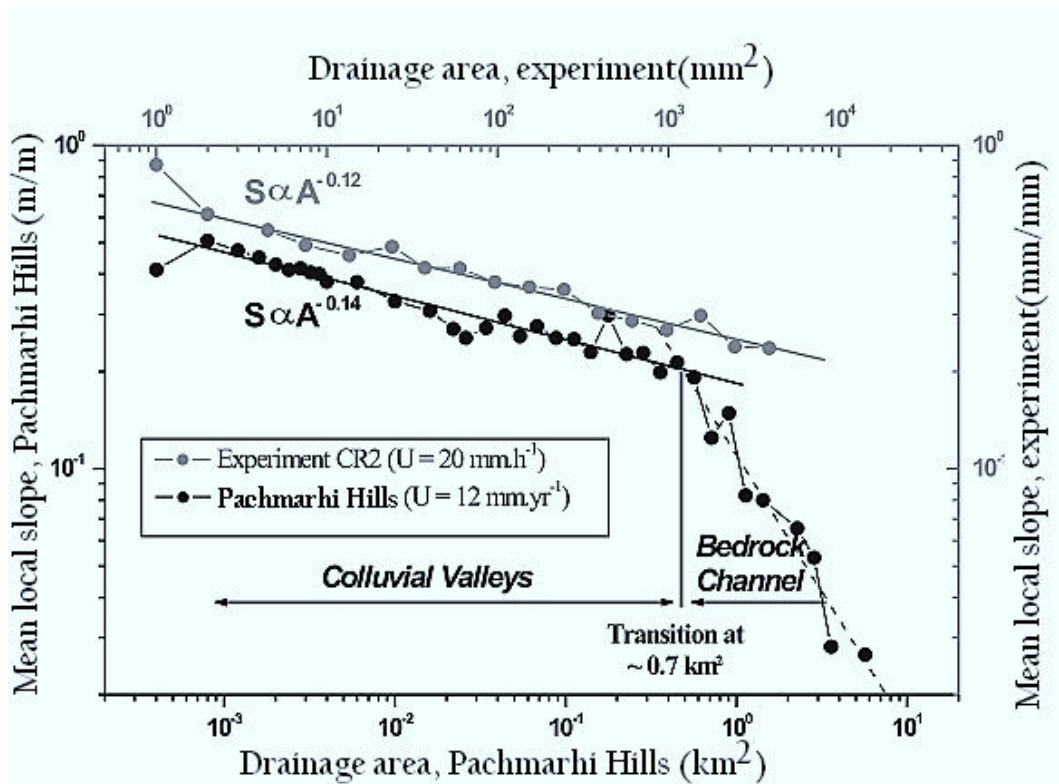

Figure 17. Slope versus drainage area in experiments and in nature. The topographic comparison is made with a small catchment located in the Pachmarhis, India.

5.3.2. Qualitative Consequences

[70] Even if erosion processes are (deliberately) oversimplified in these experiments, I have revealed some interesting relationships between elementary erosion-transport processes and macroscopic dynamic of a geomorphic system that are qualitatively relevant to the evolution of natural systems. For instance, the linear relationship I obtained between mean elevation and uplift rate has been also observed in natural systems when comparing mean elevation and mean denudation rate [*Pinet and Souriau,* 1988]. Pinet and Souriau found that the mean mechanical denudation rate of active orogens becomes negligible for a mean elevation of 500 m, suggesting that a mechanical erosion threshold exists. Moreover they also found a

linear macroscopic relationship between the mean elevation and the denudation rate, suggesting that the representative transport law also depends linearly on topographic slope. Note that this interpretation holds formally only if tectonic systems are close to, or at, dynamic equilibrium. Identical conclusions can be drawn from the linear relationship between relief and denudation rate, and the predicted ~70 m of relief remaining for null denudation rate *[Ahnert,* 1970]. These observations suggest that an erosion threshold exists at large scale in natural systems.

[71] The analysis of experimental results underlines the need to work with a large range of uplift rates in order to determine this threshold. This requirement is necessary if one wants to properly distinguish between a linear relationship with threshold, and a nonlinear one. The challenge lies in the determination of the slope exponent n, which is known to control the response time of the transient regimes of bedrock systems *[Whipple and Tucker,* 1999], and more precisely their dependency on uplift rates. The point is that, because of threshold, large steepness index are measured at small uplift rates, a behavior that would have predicted unrealistically large exponents n if no threshold is considered. This drawback has already been pointed out by *[Snyder et al.*, 2002] for bedrock channels. With our results, neglecting the threshold would lead to an erroneous slope exponent $n = 2$. This point casts some doubts on the calibration of experimental model by *Hancock and Willgoose* [2001b], where the authors neglect the detachment threshold and find a large slope exponent n^2. It might also explain the considerable differences in model parameters found by various authors.

[72] A second qualitative outcome of these experiments is about the global dynamics of tectonic and geomorphic systems. This addresses in particular the issue of how internally drained plateaus evolve when uplifted. Because of threshold, I may expect that most of erosion occurs at plateau boundaries with a dynamics that is partly controlled by river head propagation. Also the threshold may play a non negligible role in the erosion/tectonic coupling. Because of the subtle interplay between erosion and tectonics *[Avouac and Burov,* 1996; *Beaumont et al.,* 2000; *Koons,* 1989; *Willett,* 1999], I may expect that the delay between erosion and tectonics due to threshold can have some important consequences in terms of stress distribution and eventually deformation history.

6. Conclusions

[73] In this paper, I have presented new experiments on the evolution of geomorphic systems, which distinguish from previous work by the small size of the experiments, and by the use of telemetric lasers which yield to topographic measurements at an unrivalled level of precision. Using various uplift rates and initial surface shapes, I have demonstrated that topography always reaches a steady state corresponding to either a dynamic equilibrium in the case of concurrent uplift and erosion, or a resting state in the absence of uplift. The transient phase is strongly dependent on the initial surface shape, and especially on the drainage connectivity to boundary conditions. Steady state surfaces are characterized by a well-defined slope-area power law relationship with an exponent of -0.12, similar to the one estimated for fine grained alluvial channels, and collavial valleys. For a given drainage area, the eventual height limit is proportional to the uplift rate and remains significantly greater than zero in relaxation experiments. These results are consistent with a stream power law erosion model that includes a non-negligible threshold for particle detachment. I show that neglecting this threshold would have lead to erroneous parameters of the stream power law model. The study also underlines the need to deal with a large range of uplift rates in order to quantify the threshold in natural system.

[74] It is attempted to calibrate experiments with a surface-process numerical model. The key parameter appears to be the sediment transfer length which parameterizes the deposition sediment flux. The best agreement between numerical simulations and experimental results was obtained with a sediment transfer length of the order of 200 mm, which is of the experiment size.

[75] Reappraising published results on the linear dependency between mean elevation, or relief, and denudation rate, it is suggested that the derived transport model, including the erosion threshold, is worth considering for large-scale geomorphic systems. Even if our analysis is rather preliminary, it seems that a significant erosion threshold exists at large scales. Recent work on natural bedrock channels confirms this finding *[Snyder et al.,* 2002]. These results show that a detachment threshold has to be taken into account

when calibrating a stream power law model, as well as for a correct modeling of the transient dynamic of topography.

[76] Given the very high precision of our digitized topographies and the calibration of the transport and erosion law, the physical experiments can also provide strong constraints on numerical models, for which analytical solution for transient dynamics are still few.

7. Notations

Experiment Parameters

t : time since the beginning of an experiment [T].

p : precipitation rate [LT^{-1}]

U : vertica up ift rate [LT^{-1}].

RR: Relaxation experiment with random initia surface.

RE: relaxation experiment with previous y eroded initia surface.

CR: continuous uplift experiment with random initial surface.

CE: continuous uplift experiment with previously eroded initial surface.

Macroscopic Features of the Topographies

C_s: surface connectivity, dimensionless.

$C_s.ini$: initial surface connectivity, dimensionless.

$\langle h \rangle$: mean surface elevation [L].

$\langle h \rangle ini$: initial mean elevation [L].

$\langle h \rangle eq$: steady state mean elevation for continuous uplift experiments [L].

$\langle h \rangle_{lim}^{obs}$: mean elevation of the last stage of an experiment [L].

$\langle h \rangle_{lim}^{fit}$: limit mean elevation predicted from equation (1) [L].

$\langle h \rangle_u$: resting state mean surface elevation predicted from equation (2) [L].

$\langle h \rangle_{lim}$: mean surface elevation at infinite time [L]. characteristic timescale of mean elevation

τ_h: evolution calculated from mean elevation history using equation (1) [T].

τ_u: characteristic timescale of mean elevation evolution deduced from equation (2) [T].

τ: characteristic timescale of mean elevation evolution in equation (3) [T].

τ_c: characteristic timescale of connectivity evolution calculated from surface connectivity history using an exponential model [T]

Detailed Features of the Steady State Topographies

a: intercept of the steepness index-uplift rate relationship $\left[L^{2\theta}\right]$

b: slope of the steepness index-uplift rate relationship $\left[L^{2\theta-1}\,T\right]$.

A: upstream drainage area [L^2].

L: basin size computed as basin length [L].

c: Hack's law constant, dimensionless

h: local elevation [L].

x: downstream distance starting from the crest [L].

$\langle h \rangle_p$: mean profile elevation in equation 16 [L].

S: local topographic slope, dimensionless.

k: steepness index [$L2q$].

k_0: steepness index of resting state topographies $\left[L^{2\theta}\right]$

θ: slope–area exponent, dimensionless.

Physical Parameters of the Flow

Q_w: total flow discharge [L^3T^{-1}].

q_w: unit flow discharge [L^2T^{-1}].

u: flow velocity [LT^{-1}]

R: hydraulic radius [L].

d: flow depth [L]

w: flow width $[L]$.

F_r: Froude number.

R_e: Reynolds number.

v: kinematic viscosity of water or sediment– water mixture $[L^2T^{-1}]$

f: Darcy–Weisbach friction factor.

k_r: hydraulic friction factor, dimensionless.

g: gravitational acceleration $[LT^{-2}]$

α: exponent of the channel width–drainage area relationship, dimensionless.

β: constant of the channel width–drainage area relationship $[L^{2\alpha-1}]$

τ_{cr}: critical shear stress for incipient motion $[ML^{-1}T^{-2}]$.

C_v: sediment volumetric concentration, dimensionless.

ρ_w: clear water density $[ML^{-3}]$.

Erosion and Transport Laws Parameters

Q_s: total sediment flux $[L^3T^{-1}]$.

Q_c: sediment transport capacity $[L^3T^{-1}]$

E: vertical erosion rate $[LT^{-1}]$.

m, n, r: exponents of the sediment transport capacity law, dimensionless.

m', n', r': exponents of the incision law, dimensionless.

k_s: sediment transport efficiency coefficient $[L^{3(1-mr)}T^{mr-1}]$.

k_e: detachability coefficient $[L^{1-3m'}T^{m'}r'-1]$.

ξ_Q: threshold for sediment transport $[L^{3m}T^{-m}]$.

k_ξ: proportionality coefficient between ξ_Q and drainage area $[L^{3m-2}T^{-m}]$.

ξ_E: threshold for sediment detachment $[L^{3m'}T^{-m'}]$.

L_t: sediment transport length in simulation model $[L]$.

Appendix A

(A1)

[77] In case of steady uniform flow, the critical shear stress τ_{cr} for incipient motion is given by:

$$\tau_{cr} = \rho_w g(RS)_{cr} \qquad (A1)$$

where g is the gravity acceleration, ρ_w is the clear water density and R is the hydraulic radius assumed to be equal to the flow depth d, and $(RS)_{cr}$ is the depth-slope product at the onset of incipient motion. The aim is to expressed d in terms of slope and drainage area. The unit flow discharge q_w is equal to:

$$q_w = ud = \frac{pA}{w}, \qquad (A2)$$

where u is the mean flow velocity. If it is assumed a power law relationship between channel width and drainage area of the form:

$$w = \beta A^\alpha, \qquad (A3)$$

then:

$$q_w = \frac{p}{\beta} A^{1-\alpha} \qquad (A4)$$

[78] In the case of laminar flow, u is given by the Darcy-Weisbach formula:

$$u = \sqrt{\frac{8g}{f} dS}, \qquad (A5)$$

where f is the Darcy-Weisbach friction factor, which can also be expressed in function of the Reynolds

Number *Re:*

$$f = k_r/R_e = \frac{k_r v}{ud} = \frac{k_r v}{qw}, \tag{A6}$$

where k_r is a dimensionless roughness factor. Substituting (A4) into (A6), and then (A6) into (A5) gives:

$$d = \left(\frac{pk_r v}{8g\beta} \frac{A^{1-\alpha}}{S}\right)^{1/3}, \tag{A7}$$

which when recast into equation (A1), gives the following expression for the area-slope relationship of resting state in the case of relaxation experiments:

$$S = \frac{\tau_{cr}^{3/2}}{g\rho_w^{3/2}} \left(\frac{8\beta}{pk_r v}\right)^{1/2} A^{\frac{1-0}{2}}, \tag{A8}$$

References

- Ahnert, F., 1970 Functional relationships between denudation, relief, and uplift in large mid-latitude drainage basins, *Am. J. Sci., 268,* 243-263,.
- Ashmore, P. E., 1982 Laboratory modelling of gravel braided stream morphology, *Earth Surf Processes Landforms, 7,* 201-225,.
- Avouac, J. P., and E. B. Burov, 1996 Erosion as a driving mechanism of intra-continental mountain growth, *J. Geophys. Res.,* 101(B8), 17,74717,769,.
- Beaumont, C., P. Fullsack, and J. Hamilton, 1992 Erosional control of activecompressional orogens, in *Thrust Tectonics,* edited by K. R. McClay, pp. 1-18, Chapman and Hall, New York,.
- Beaumont, C., H. Kooi, and S. Willett, Coupled tectonic-surface process models with applications to rifted margins and collisional orogens, in *Geomorphology and Global Tectonics,* edited by M. A. Summerfield, pp. 29-55, John Wiley, New York, 2000.
- Braun, J., and M. Sambridge, 1997 Modelling landscape evolution on geological time scales: A new method based on irregular spatial discretization, *Basin Res., 9,* 27-52,.
- Coussot, P., 1997 *Mudflow Rheologyand Dynamics,* A. A. Balkema, Brookfield, Vt.,.
- Crave, A., and P. Davy, A 2001stochastic "precipiton" model for simulating erosion/sedimentation dynamics, *Comput. Geosci., 27,* 815-827,.
- Crave, A., D. Lague, P. Davy, J. Kermarrec, D. Sokoutis, L. Bodet, and R. Compagnon, 2000 Analogue modelling of relief dynamics, *Phys. Chem. Earth, Part A,* 25(6-7), 549-553,.
- Czirok, A., E. Somfai, and T. Vicsek, 1993 Experimental evidence for self-affine roughening in a micromodel of geomorphological evolution, *Phys. Rev. Lett.,* 71(13), 2154-2157,.
- Darboux, F., P. Davy, C. Gascuel-Odoux, and C. Huang, 2002 Evolution of soil surface roughness and flowpath connectivity in overland flow experiments, *Catena,* 46(2-3), 125-139,.
- Davy, P., and P. Cobbold, 1991 Experiments on shortening of a 4 layer model of continental lithosphere, *Tectonophysics, 188,* 1-25,.
- Davy, P., and A. Crave, 2000 Upscaling local-scale transport processes in large-scale relief dynamics, *Phys. Chem. Earth, Part A,* 25(6-7), 533-541,.
- Densmore, A. L., R. S. Anderson, B. G. McAdoo, and M. A. Ellis, 1997 Hill-slope evolution by bedrock landslides, *Science, 275,* 369 -372,.
- Densmore, A. L., M. A. Ellis, and R. S. Anderson, 1998Landsliding and the evolution of normal fault-bounded mountain ranges, *J. Geophys. Res.,* 103(B7), 15,203-15,219,.
- Flint, J. J., 1973 Experimental development of headward growth of channel networks, *Geol. Soc. Am. Bull., 84,* 1087-1094,.
- Flint, J.-J., 1974 Stream gradient as a function oforder magnitude, and discharge, *Water Resour. Res.,* 10(5), 969-973,.
- Gardner, T. W., 1983 Experimental study of knickpoint and longitudinal profile evolution in cohesive, homogeneous material, *Geol. Soc. Am. Bull., 94,* 664-672,.
- Govers, G., 1992Evaluation of transporting capacity formulae for overland flow, in *Overland Flow: Hydraulics and Erosion Mechanics,* edited by A. J. Parsons and A. D. Abrahams, pp. 243 -273, UCL Press, London, a.
- Govers, G., 1992 Relationship between discharge, velocity and flow area for rills eroding loose, non-layered materials, *Earth Surf. Processes Landforms,* 17, 515-528, b.

- Hack, J. T., 1957 Studies of longitudinal stream profiles in Virginia and Maryland, *U. S. Geol. Surv. Prof Pap., 294B,* 45-94,.
- Hack, J. T., 1960 Interpretation of erosional topography in humid temperate regions, *Am. J. Sci., 258,* 80-97,.
- Hairsine, P. B., and C. W. Rose, 1992 Modeling water erosion due to overland flow using physical principles, 1, Sheet flow, *Water Resour. Res. , 28*(1), 237-243,.
- Hancock, G., and G. Willgose, 2001The production of digital elevation models for experimental model landscapes, *Earth Surf. Processes Landforms, 26,* 475 -490, a.
- Hancock, G., and G. Willgoose, 2001Use of a landscape simulator in the validation of the SIBERIA catchment evolution model: Declining equilibrium landforms, *Water Resour. Res.,* 37(7), 1981-1992, b.
- Hasbargen, L. E., and C. Paola, 2000 Landscape instability in an experimental drainage basin, *Geology, 28*(12), 1067-1070,.
- Holland, W. N., and G. Pickup, 1976 Flume study of knickpoint development in stratified sediment, *Geol. Soc. Am. Bull., 87,* 76-82,.
- Howard, A. D., 1980 Thresholds in river regimes, in *Thresholds in Geomorphol-ogy,* edited by D. R. Coates and J. D. Vitek, pp. 227 -258, Allen and Unwin, Concord, Mass.,.
- Howard, A. D., 1994 A detachment-limited model of drainage basin evolution., *Water Resour. Res., 30*(7), 2261 -2285,.
- Howard, A. D., 1998Long profile development of bedrock channels: Interaction of weathering, mass wasting, bed erosion and sediment transport, in *Rivers Over Rock: Fluvial Processes in Bedrock Channels, Geophys. Monogr. Ser.,* $vol. 107, edited by K. J. Tinkler and E. E. Wohl, pp.$ 297-319, AGU, Washington, D.C.,.
- Howard, A. D., and G. Kerby, 198 Channel changes in badlands, *Geol. Soc. Am.*
- *Bull., 94,* 739-752, 3.
- Howard, A. D., W. E. Dietrich, and M. A. Seidl, 1994 Modeling fluvial erosion on regional to continental scales, *J. Geophys. Res. , 99*(B7), 13,971 -13,986,.
- Hurtrez, J.-E., F. Lucazeau, J. Lave, and J.-P. Avouac, 1999 Investigation of the relationships between basin morphology, tectonic uplift, and denudation from the study of an active fold belt in the Siwalik Hills, central Nepal, *J. Geophys. Res.,* 104(B6), 12,779-12,796,.
- Ijjasz-Vasquez, E. J., and R. L. Bras, 1995 Scaling regimes of local slope versus contributing area in digital elevation models, *Geomorphology, 12,* 299311,.
- Kirkby, M. J., 1971Hillslope process-response models based on the continuity equation, *Spec. Publ. Inst. Br. Geogr., 3,* 15-30,.
- Kooi, H., and C. Beaumont, 1996Large-scale geomorphology: Classical concepts reconciled and integrated with contemporary ideas via a surface processes model, *J. Geophys. Res., 101*(B2), 3361 -3386,.
- Koons, P. O., 1989The topography evolution of collisional moutain belts: A numerical look at the southern Alps New-Zealand, *Am. J. Sci., 289,* 1041-1069,.
- Lague, D., P. Davy, and A. Crave, 2000 Estimating uplift rate and erodibility from the area-slope relationship: Examples from Brittany (France) and numerical modelling, *Phys. Chem. Earth, Part A, 25*(6 -7), 543 -548,
- Lave, J., and J. P. Avouac, 2001 Fluvial incision and tectonic uplift across the Himalayas of central Nepal, *J. Geophys. Res.,* 106(B11), 26,561-26,591,.
- Lague, Dimitri. Crave, Alain. Davy, Philippe. , 2003 Laboratory experiments simulating the geomorphic response to tectonic uplift Journal of Geophysical Research   Vol 108 Issue
- Leopold, L. B., and T. J. Maddock, 1953The hydraulic geometry of stream channels and some physiographic implications, *U. S. Geol. Surv. Prof. Pap., 252,* 57,.
- Meunier, P., and F. Metivier, 2000 Permanence des fluxs de masse d'une riviereen tresses experimentales, *C. R. Acad. Sci. Paris, Earth Planet. Sci., 331,*105-110,.
- Mizutani, T., 1998 Laboratory experiment and digital simulation of multiple fill-cut terrace formation, *Geomorphology, 24,* 353-361,.
- Moglen, G. E., and R. L. Bras, 1995 The effect of spatial heterogeneities on geomorphic expression in a model of basin evolution, *Water Resour.Res.,* 31(10), 2613-2623,.
- Molnar, P., 2001 Climate change, flooding in arid environments, and erosion rates, *Geology,* 29(12), 1071-1074,.

- Montgomery, D. R., 2001 Slope distributions, threshold hillslopes, and steady-state topography, *Am. J. Sci., 301,* 432-454,.
- Montgomery, D. R., and E. Foufoula1993-Georgiou, Channel network source representation using digital elevation models, *Water Resour. Res., 29*(12), 3925-3934,.
- Montgomery, D. R., and K. B. Gran, 2001 Downstream variations in the width of bedrock channels, *Water Resour. Res., 37*(6), 1841 -1846,.
- Paola, C., G. Parker, R. Seal, S. K. Sinha, J. B. Southard, and P. R. Wilcock, 1992 Downstream fining by selective deposition in a laboratory flume, *Science,* 258, 1757-1760,.
- Phillips, L. F., and S. A. Schumm, 1987 Effect of regional slope on drainagenetworks, *Geology, 15,* 813-816,.
- Pinet, P., and M. Souriau, 1988 Continental erosion and large-scale relief, *Tectonics, 7*(3), 563 -582,.
- Rigon, R., I. Rodriguez-Iturbe, A. Maritan, A. Giacometti, D. G. Tarboton, and A. Rinaldo, 1996 On Hack's law, *Water Resour. Res.,* 32(11), 3367-3374,
- Rinaldo, A., W. E. Dietrich, R. Rigon, G. K. Vogel, and I. Rodriguez-Iturbe, 1995 Geomorphological signatures ofvarying climate, *Nature, 374,* 632-635,.
- Roering, J. J., J. W. Kirchner, L. S. Sklar, and W. E. Dietrich, 2001Hillslope evolution by nonlinear creep and landsliding: An experimental study,*Geology, 29*(2), 143 -146,.
- Salles, C., J. Poesen, and G. Govers, 2000 Statistical and physical analysis ofsoil detachment by raindrop impact: Rain erosivity indices and thresholdenergy, *Water Resour. Res., 36*(9), 2721 -2729,.
- Schorghofer, N., and D. H. Rothman, 2001Basins of attraction on random topography, *Phys. Rev. E, 63*(026), 112,.
- Schorghofer, N., and D. H. Rothman, 2002 Acausal relations between topographic slope and drainage area, *Geophys. Res. Lett., 29*(13), 1633, doi:10.1029/2002GL015144,.
- Schumm, S. A., M. P. Mosley, and W. E. Weaver, 1987 *Experimental Fluvial Geomorphology,* John Wiley, New York,.
- Seidl, M. A., and W. E. Dietrich, 1992The problem of channel erosion into bedrock, *Catena Suppl., 23,* 101-124,.
- Sharma, P. P., S. C. Gupta, and W. J. Rawls, 1991Soil detachment by single raindrops of varying kinetic energy, *Soil Sci. Soc. Am. J., 55,* 301-307,.
- Sheperd, R. G., and S. A. Schumm, 1974 Experimental study of river incision, *Geol. Soc. Am. Bull., 85,* 257-268,.
- Sklar, L., and W. E. Dietrich, 1998 River longitudinal profiles and bedrock incision models: Stream power and the influence of sediment supply, in *Rivers Over Rock: Fluvial Processes in Bedrock Channels, Geophys. Monogr. Ser.,* vol. 107, edited by K. J. Tinkler and E. E. Wohl, pp. 237-260, AGU, Washington, D.C.,.
- Sklar, L. S., and W. E. Dietrich, 2001 Sediment and rock strength controls on river incision into bedrock, *Geology,* 29(12), 1087-1090,.
- Smith, C. E., 1998Modeling high sinuosity meanders in a small flume, *Geomor-phology, 25,* 19-30,.
- Smith, T. R., and F. P. Bretherton, 1972 Stability and the conservation of mass in drainage basin evolution, *Water Resour. Res., 8*(6), 1506-1529,.
- Snyder, N. P., 2001Bedrock channel response to tectonic, climatic, and eustatic forcing, Ph.D thesis, Dep. of Earth, Atmos., and Planet. Sci., Mass. Inst.of Technol., Cambridge, Mass.,.
- Snyder, N. P., K. X. Whipple, G. E. Tucker, and D. J. Merritts, 2000 Landscape response to tectonic forcing: DEM analysis of stream profiles in theMendocino triple junction region, northern California, *Geol. Soc. Am.Bull., 112,* 1250-1263,.
- Snyder, N. P., K. X. Whipple, G. E. Tucker, and D. J. Merritts, 2002Channel response to tectonic forcing: Field analysis of stream morphology and hydrology in the Mendocino triple junction region, northern California, *Geomorphology,* in press,.
- Talling, P. J., 2000 Self-organization of river networks to threshold states, *Water Resour. Res.,* 36(4), 1111-1128,.
- Tarboton, D. G., 1997 A new method for the determination of flow directions and contributing areas in grid digital elevation models, *Water Resour. Res., 33*(2), 309-319,.
- Tarboton, D. G., R. L. Bras, and I. Rodriguez-Iturbe, 1989 Scaling and elevation in river networks, *Water Resour. Res., 25*(9), 2037-2051,.

- Tarboton, D. G., R. L. Bras, and I. Rodriguez-Iturbe, 1992 A physical basis for drainage density, *Geomorphology, 5,* 59-76,.
- Thompson, D., and E. Wohl, 1987 Flume experimentation and simulation of bedrock channel processes, in *Rivers Over Rock: Fluvail Processes in Bedrock Channels, Geophys. Monogr. Ser.,* vol. 107, edited by K. J. Tinkler and E. E. Wohl, pp. 279-296, AGU, Washington, D.C., 1998. Torri, D., M. Sfalanga, and G. Chisci, Threshold conditions for incipient rilling, *Catena Suppl., 8,* 97-105,.
- Tucker, G. E., and R. L. Bras, 1998 Hillslope processes, drainage density, and landscape morphology, *Water Resour. Res.,* 34(10), 2751-2764,.
- Tucker, G. E., and R. L. Bras, 2000 A stochastic approach to modeling the role of rainfall variability in drainage basin evolution, *Water Resour. Res.,* 36(7), 1953-1964,.
- Tucker, G. E., and R. Slingerland, 1996 Predicting sediment flux from fold and thrusts belts, *Basin Res.,* 329-349,.
- Tucker, G. E., and R. Slingerland, 1997 Drainage basin response to climate change, *Water Resour. Res.,* 33(8), 2031-2047,.
- Tucker, G. E., and K. X. Whipple, 2002Topographic outcomes predicted by stream erosion models: Sensitivity analysis and intermodel comparison,*J. Geophys. Res.,* 107(B9), 2179, doi: 10.102 9/ 2001 JB000162,.
- Tucker, G. E., S. T. Lancaster, N. M. Gasparini, and R. L. Bras, 2001 The channel-hillslope integrated model (CHILD), in *Landscape Erosion and Evolution Modeling,* edited by R. S. Harmonand and W. W. I. Doe, pp. 349-388, Kluwer Acad., Norwell, Mass.,. Vandaele, K., J. Poesen, G. Govers, and B. van Wesemael, Geomorphic threshold conditions for ephemeral gully incisions, *Geomorphology, 16,*161-173, 1996.
- Whipple, K. X., 2001 Fluvial landscape response time: How plausible is steady-state denudation?, *Am. J. Sci., 301,* 313-325,.
- Whipple, K. X., and G. E. Tucker, 1999 Dynamics of the stream-power river incision model: Implications for height limits of mountain ranges, landscape response timescales, and research needs, *J. Geophys. Res.,* 104(B8), 17,661-17,674,.
- Whipple, K. X., and G. E. Tucker, 2002Implications of sediment-flux-dependent river incision models for landscape evolution, *J. Geophys. Res.,* 107(B2),.
- Whipple, K. X., G. Parker, C. Paola, and D. Mohrig, 1998 Channel dynamics, sediment transport, and the slope of alluvial fans: Experimental study, *J. Geol., 106,* 677-693,.
- Willett, S. D., 1999 Orogeny and orography: The effects of erosion on the structure of mountain belts, *J. Geophys. Res.,* 104(B12), 28,957-28,982,.
- Willgoose, G., R. L. Bras, and I. Rodriguez-Iturbe, 1991 A physical explanation of an observed link area-slope relationship, *Water Resour. Res.,* 27(7), 1697-1702, a.
- Willgoose, G., R. L. Bras, and I. Rodriguez-Iturbe, 1991 Results from a new model of river basin evolution, *Earth Surf Processes Landforms, 16,*237-254, b.
- Wittmann, R., T. Kautzky, A. Hubler, and E. Liischer, 1991 A simple experiment for the examination of dendritic river systems, *Naturwissenschaften, 78,* 23-25,.
- Wood, L. J., F. G. Ethridge, and S. A. Schumm, 1993 The effects of rate of base-level fluctuation on coastal-plain, shelf and slope depositional systems: An experimental approach, *Spec. Publ. Int. Ass. Sediment., 18,* 43-53,
- Crave and P. Davy, Geosciences Rennes, UMR 6118 CNRS, Campus de Beaulieu, 35042 Rennes, cedex, France.
- D. Lague, Department of Earth Sciences, University of Cambridge, Downing Street, Cambridge CB2 3EQ, UK. (dlag02@esc.cam.ac.uk)